Journal of Geophysical Research: Biogeosciences

RESEARCH ARTICLE
10.1029/2017JG004347

On Upscaling of Soil Microbial Processes and Biogeochemical Fluxes From Aggregates to Landscapes

Ali Ebrahimi[1] and **Dani Or**[1]

[1]Department of Environmental Systems Science, ETH Zürich, Zürich, Switzerland

Key Points:
- We report a mechanistic and analytical modeling framework for integrating local environmental effects on GHG-producing microbial processes
- The mechanistic model enables evaluation of how structural features, spatial variability, and ambient conditions affect microbial functioning
- The modeling framework was evaluated using field data for seasonal N_2O emissions from subarctic regions resulting in good agreement

Supporting Information:
- Supporting Information S1

Correspondence to:
A. Ebrahimi,
ali.ebrahimi@usys.ethz.ch

Citation:
Ebrahimi, A., & Or, D. (2018). On upscaling of soil microbial processes and biogeochemical fluxes from aggregates to landscapes. *Journal of Geophysical Research: Biogeosciences*, *123*, 1526–1547. https://doi.org/10.1029/2017JG004347

Received 1 DEC 2017
Accepted 12 APR 2018
Accepted article online 24 APR 2018
Published online 11 MAY 2018

Abstract Soil microbial communities respond to spatial and temporal variations in environmental conditions (e.g., saturation and ambient temperatures) as reflected in the dynamics of microbially produced greenhouse gas (GHG) fluxes (primarily CO_2, N_2O, and CH_4) emitted from soil surfaces. Despite considerable progress in resolving key soil microbial processes, their quantification remains largely empirical with limited predictability. We report a mechanistic and analytical modeling framework for integrating local environmental effects on GHG-producing microbial processes primarily in soil aggregates (or other hot spots) and the upscaling of these to regional GHG fluxes. The mechanistic model enables systematic evaluation of how soil structural features (e.g., aggregation and layers), spatial variability, and dynamic ambient conditions (e.g., temperature and hydration) affect soil microbial functioning. The upscaling of microbial processes from aggregates of different sizes to soil profiles and landscapes implements mechanistically derived microbial response functions with spatial information on soil type, land cover, and resource distribution. The modeling framework was evaluated using reported field data for seasonal N_2O emissions from subarctic regions resulting in reasonable agreement. The proposed analytical framework offers a practical compromise balancing a simplified representation of dynamic microbial processes that respond to local conditions with an upscalable representation of soil GHG fluxes over landscapes under changing environmental conditions.

1. Introduction

The composition and structure of microbial communities is considered important for various facets of soil ecological and biogeochemical functioning (Azam, 1998; Bardgett et al., 2008; Ebrahimi, 2017; Morales et al., 2010; Schimel & Schaeffer, 2012). In the context of climate change, the emission of greenhouse gases (GHG) from organic soils such as peatlands and thawing permafrost are of particular importance due to the large amounts of stored soil organic carbon and nitrogen (Bousquet et al., 2006; IPCC, 2014; Jansson & Taş, 2014; Natali et al., 2011). Special attention has been given to soil biogeochemical gases produced by anaerobic soil microbial processes (e.g., N_2O and CH_4); these are considered as potent GHG sources due to their strong photochemical atmospheric interactions (Hansen et al., 2000; Meinshausen et al., 2009). Observations of spatially variable and highly dynamic rates of soil GHG emissions affect the uncertainty in climate change projection especially with the intricacies of hydroclimatic feedbacks (e.g., permafrost thaw, droughts, or frequent floods).

The relative importance of environmental factors such as soil heterogeneity (e.g., texture and aggregation), resource spatial distribution (carbon and nitrate), and dynamic hydration conditions on microbial processes and biogeochemical reactions is relatively well understood, at least in a qualitative sense (Ebrahimi & Or, 2014, 2015; Nunan et al., 2003, 2007; Tiedje et al., 1984; Young & Crawford, 2004). To date, many of the qualitative and conceptual insights regarding microbial interactions in natural soils have not been transformed into mechanistic and quantitative frameworks that could offer predictive capabilities at practical scales of interest. Biogeochemical modules in Earth system models often consider soil microbial activity by assuming a linear relationship between soil C and N stocks and the emitted GHG fluxes (Schimel, 2001; Wieder et al., 2015). Some process-based models have described soil gas fluxes by calibration based on field-scale flux observations using parameters derived from long-term incubation experiments to assign various pools of carbon and nitrogen stocks (McGuire et al., 2001; Molina-Herrera et al., 2016; Murguia-Flores et al., 2017; Pumpanen et al., 2003). Other models link the conceptual pools of microbial biomass with GHG production and emissions using empirical first-order linear decay rates (some include environmental factors; Manzoni et al., 2014; Sierra et al., 2012; Wu et al., 2015). While parameterizations by conceptual pools enhanced our

understanding on the dynamics of carbon and nitrogen stocks, their limited links with mechanistic and measurable quantities makes it difficult to consider soil structural features and resource spatial distributions that are known to play important roles in regulating net GHG emissions from soil (Sierra et al., 2011; Smith et al., 2002; Wieder et al., 2015).

Evidence suggests that several abiotic factors play a dominant role in controlling soil microbial processes and associated GHG emission rates and patterns (Ebrahimi & Or, 2016; Manzoni et al., 2014; Tecon & Or, 2017). Motivated by these observations and evidences, we have developed mechanistic models that consider microbial community dynamics and variations in resource utilization in response to changes in soil and other environmental factors to better link biogeochemical interactions with large-scale hydrologic-climatic processes (Ebrahimi & Or, 2015; Kim & Or, 2017; Vogel et al., 2015). The parameterization of such mechanistic models remains a challenge, and observational capabilities lag behind. Moreover, the computational burden becomes prohibitive for detailed model application at large scales of practical interest. We thus seek a modeling framework that retains salient responses of microbial activity with changes in micro-environmental conditions (without the burden of explicitly representing such micro-environments). We seek a simple model that retains dynamic response and capable of linking microbial processes from aggregates and soil profile to regional-scale fluxes at moderate computational and parameterization needs.

Motivated by this goal, the specific objectives were to (1) develop an analytical model based on idealized spherical aggregates that integrates interactions between soil aggregates and oxygen content in formation of anoxic microsites for anaerobic microbial activity, (2) integrate microbial response functions from a detailed biophysical model for an aggregate and upscale the aggregate model to soil profiles for estimation of profile-scale GHG emissions, (3) expand the model to regional scales using land cover maps and regional-scale heterogeneities of soil texture and resource distributions, and (4) evaluate the model response to seasonal and spatial variations on N_2O gas emissions and compare with field observations.

2. Theoretical Considerations

We expand a previously developed analytical model that considers conditions within spherical soil aggregates and the onset of anaerobic microbial hot spots in a soil matrix under certain conditions (Ebrahimi & Or, 2015; Smith, 1980). Aggregates are drawn from a statistical population of different sizes (similar to reported in natural soils). Aggregate assemblies of different sizes populate different depths/layers of a soil profile and are subjected to different macroscopic hydration and aeration boundary conditions (Ebrahimi & Or, 2016). The model then considers microbial processes across a range of spatial and temporal environmental conditions, from individual aggregates ("hot spot") to soil profiles and regions composed of many soil profiles with different characteristics (Ebrahimi & Or, 2016; Gupta & Germida, 2015; Kuzyakov & Blagodatskaya, 2015; Nunan et al., 2007; Or et al., 2007).

For simplicity, we consider an idealized soil aggregate as the basic modeling building blocks, where details of microbial self-organization and community functioning are simplified and parameterized based on results compiled from detailed pore-scale model (Ebrahimi & Or, 2015, 2016;). In essence, we have consolidated information from a numerical model that explicitly represents microbial life in soil pore networks considering individual cell activity (e.g., dispersion, nutrient uptake, growth, division, and death) across a range of conditions that we varied systematically (Borer et al., 2018; Ebrahimi & Or, 2015; Kim & Or, 2016; Wang & Or, 2014). The results were used to derive aggregate microbial functions that are used as inputs into an analytical aggregate model. The fluxes from idealized soil aggregates (different sizes and depths) were integrated to provide estimates of GHG fluxes from soil profiles (see Figure 1 for schematic representation of the modeling and upscaling strategies). Different profile-scale fluxes are estimated from different units in the landscape and weighted to estimate regional GHG surface fluxes using spatial maps of soil and land cover attributes and relevant hydroclimatic information.

2.1. Biogeochemical Processes at Individual (Hot Spot) Aggregate Level

Microbial hot spots may form in soil aggregates under certain conditions; such concentrated regions of microbial activity may become anoxic and affect a wide range of biogeochemical processes (Ananyeva et al., 2013; Philippot, 1996; Six et al., 1998; Tiedje et al., 1983). For generality, we consider an idealized model of a spherical "aggregate" as a representative generic hot spot where anaerobic conditions emerge due to microbial activity and inhibited oxygen diffusive fluxes into such microenvironments (see Borer et al., 2018;

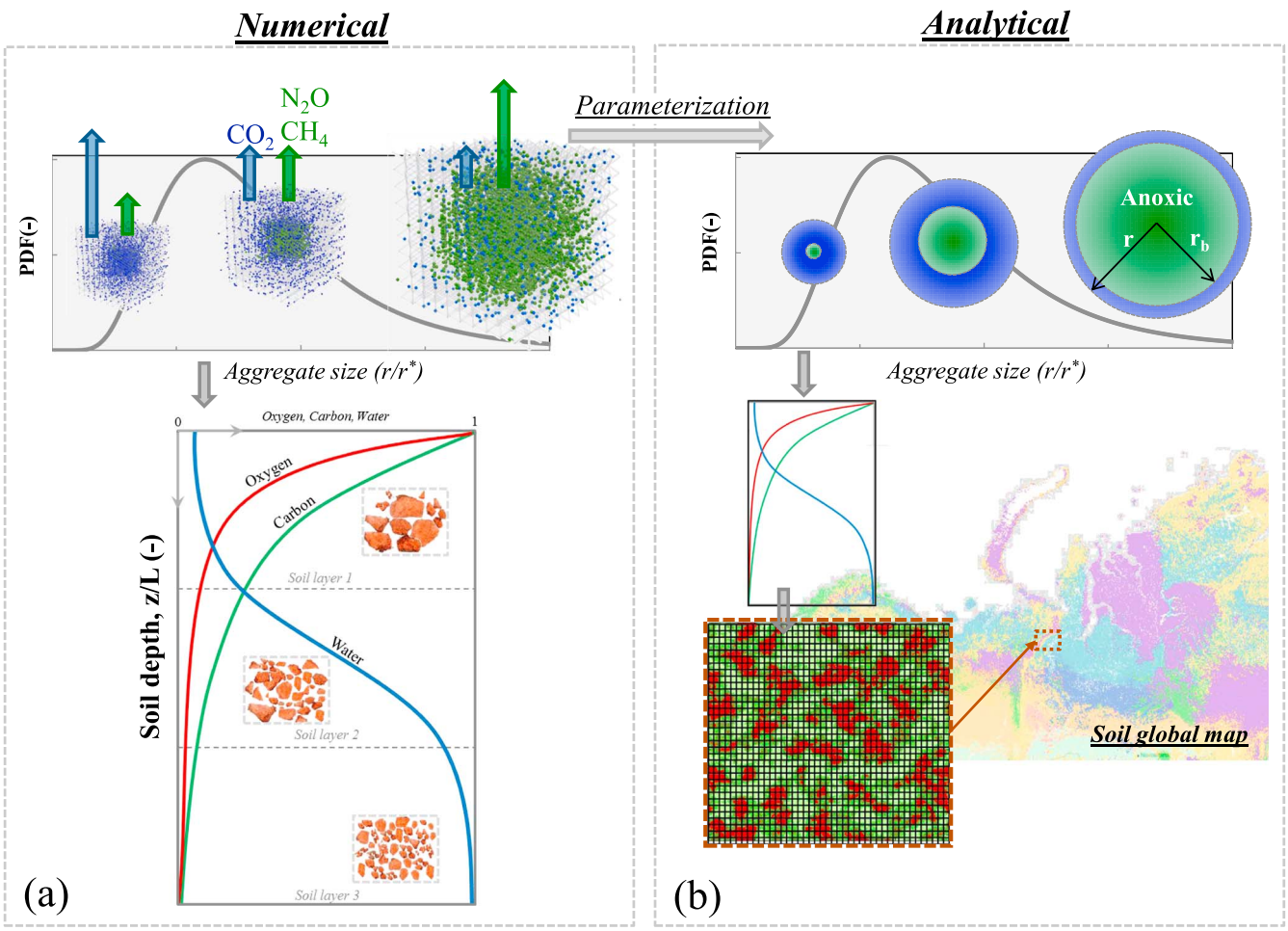

Figure 1. Schematic of analytical modeling procedure parameterized through numerical pore-scale modeling. (a) Numerical modeling of microbial aerobic (blue dots) and anaerobic (green dots) activities from single aggregates of different size classes to soil profile with variations of local macroscopic boundary conditions for oxygen, and carbon concentrations and water saturation as functions of soil depth. (b) Analytical modeling procedure of GHG fluxes from idealized spherical aggregates to soil profile and regional scales where soil physical and chemical properties spatially vary. Soil global map obtained from (Hengl et al., 2017).

Ebrahimi & Or, 2015; Sexstone et al., 1985; Tiedje et al., 1984). Evidence suggests that such microenvironments (often of millimetric scales) may host dense microbial communities with own local trophic interactions (Briar et al., 2011; Cosentino et al., 2006; Nie et al., 2014).

Considering a prototypic spherical soil aggregate, a simple analytical model for steady-state radial oxygen diffusion reaction (microbial) is expressed as follows:

$$D_{\text{eff.}}\left(\frac{\mathrm{d}^2[\mathrm{O}_2]}{\mathrm{d}r^2}+(2/r)\frac{\mathrm{d}[\mathrm{O}_2]}{\mathrm{d}r}\right)=Q^m_{[\mathrm{O}_2]} \tag{1}$$

where r (m) is the aggregate radius. $Q^m_{[\mathrm{O}_2]}$ (g hr^{-1} m^{-3}) is the mean volumetric oxygen consumption rate per aggregate due to microbial activity. The function $Q^m_{[\mathrm{O}_2]}$ encapsulates the response of microbial community structure and functioning that may be influenced by factors such as aggregate size and pore network characteristics, hydration conditions, temperature, and organic carbon content (Arah & Smith, 1989). A central goal of this study is to propose a systematic parameterization scheme for quantifying these volumetric microbial consumption rate functions (Q^m) based on detailed individual-based models of microbial life in pore network model for a range of conditions. As described in section 2.2 (Figures 2 and 3), Q^m is a function of dissolved organic matter content, oxygen concentration at aggregate surface, and aggregate size.

The solution of equation (1) for a prescribed microbial consumption rate $Q^m_{[\mathrm{O}_2]}$ requires two boundary conditions; these could be represented either by (1) a constant oxygen concentration ($[\mathrm{O}_2]^b$ [mg/L]) at the

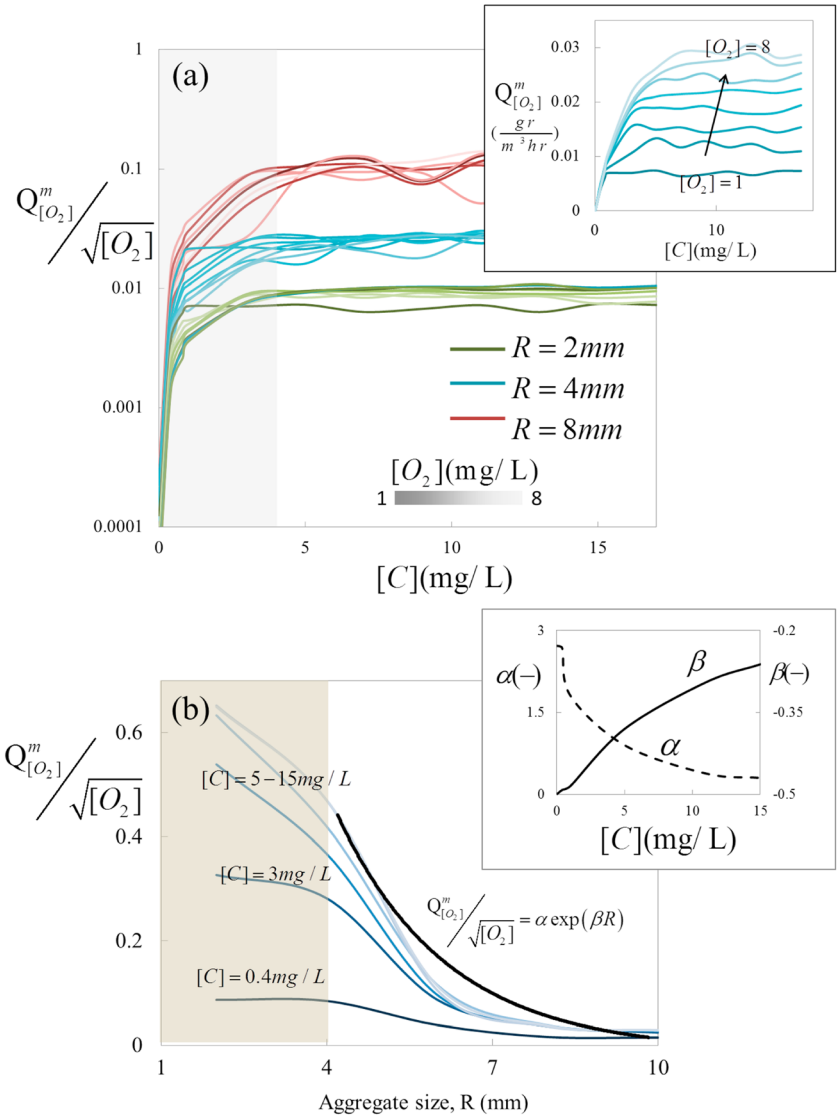

Figure 2. (a) Normalized mean uptake rate of oxygen required for the analytical model as a function of carbon and oxygen contents. Inset figure shows the effects of oxygen content on its mean uptake rate. (b) Effects of aggregate size on normalized oxygen uptake rate as deduced from numerical results of microbial communities grown in the pore network model. Solid black line represents the fitted model on numerical data. The fitting parameters for the power law relationship of the mean oxygen uptake rate as a function of aggregate size are shown in the inset figure (b).

aggregate surface that is obtained from macroscopic boundary conditions over the soil depth or by (2) zero oxygen flux at the aggregate radius equal to the size of the anoxic zone (r_{an} [m]) where oxygen consumption becomes zero. The analytical solution of equation (1) provides the oxygen concentration profile O_2 (mg/L or g/m^3) along the aggregate radius, expressed as follows:

$$O_2(r) = [O_2]_b + \frac{Q^m_{[O_2]}}{6D_{eff.}}\left[(R^2 - r^2) - 2r^3_{an}\left(\frac{1}{r} - \frac{1}{R}\right)\right] \quad (2)$$

The size of the anoxic zone within individual aggregates (r_{an}) could be then obtained as a function of aggregate size (R [m]) by finding where the oxygen flux (derivative of equation (2)) vanishes ($\frac{\partial O_2(r)}{\partial r}\Big|_{r = r_{an}} = 0$). The explicit expression is given as follows:

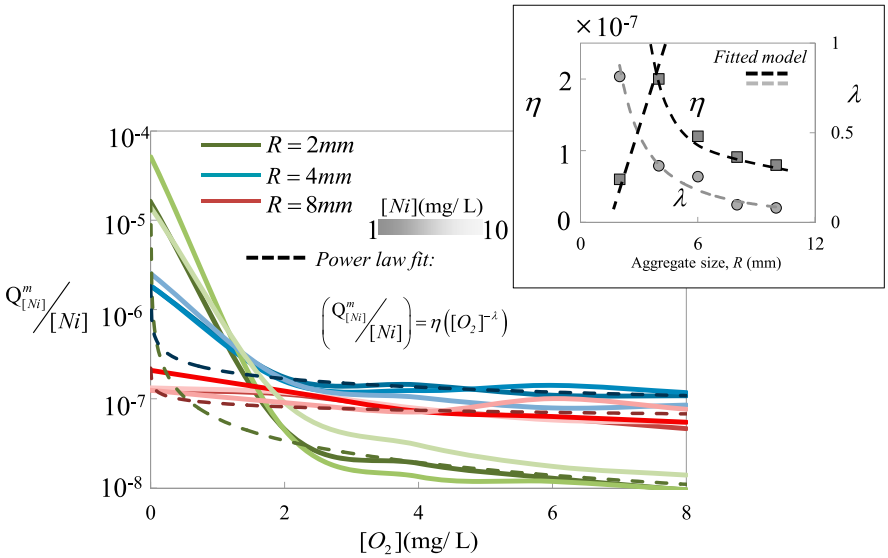

Figure 3. Mean nitrate volumetric uptake rate ($Q_{[Ni]m}$) normalized by nitrate concentration [Ni], required for the analytical model as a function of oxygen content, shown for three aggregate sizes. Effects of aggregate size on normalized nitrate uptake rate is deduced from numerical results of microbial anaerobic communities simulated in pore network model (Ebrahimi & Or, 2016). Dashed lines represent the fitted power law model on numerical data of normalized nitrate uptake rate. The fitting parameters of power law relationship are represented in the inset figure.

$$1 - 3\left(\frac{r_{an}}{R}\right)^2 + 2\left(\frac{r_{an}}{R}\right)^3 = \frac{1}{\sqrt{3}R}\left(\frac{6D_{eff.}[O_2]^b}{Q^m_{[O_2]}}\right)^{1/2} \tag{3}$$

We use the oxygen profile (equation (2)) and the size of the anoxic zone within an individual aggregate (equation (3)) to estimate the potential for microbially produced GHG fluxes, as described in the following and represented schematically in Figure S1.

The net respiration flux of CO_2 per aggregate of a certain size is calculated based on a stoichiometric coefficient, $a_{sto.}$ (depending on carbon source), aggregate size (R), and the mean volumetric oxygen uptake rate, $Q^m_{[O_2]}$ as follows:

$$V_{CO_2} = \left(\frac{4}{3}\pi R^3\right) a_{sto} Q^m_{[O_2]} \tag{4}$$

V_{CO_2} accounts for CO_2 flux for the conditions where carbon resides within soil aggregates and consumed by aerobic and anaerobic microbial communities. It should be noted that in addition to these specific "hot spots," gas fluxes from background carbon pools of the soil matrix are included, as discussed in section 2.3.

For other anaerobically produced GHG, the information on oxygen distribution and content is required to estimate production rates. For example, N_2O production occurs only when the oxygen content in the anoxic zone of an aggregate is above a critical threshold ($[O_2] > [O_2]_c$), where $[O_2]_c$ (mg/L) is the threshold oxygen content (about 2% of atmospheric level) below which N_2O is consumed and converted to N_2 (Bouwman, 1998; Morley et al., 2008; Morley & Baggs, 2010). Therefore, N_2O gas fluxes from denitrification process are quantified using the following conditional equation:

$$\begin{cases} V_{N_2O} = \left(\frac{4}{3}\pi R^3\right) a^{Ni}_{sto} Q^m_{[Ni]}, & [O_2] > [O_2]_c \\ V_{N_2O} = 0, & [O_2] < [O_2]_c \end{cases} \tag{5}$$

where $Q_{[Ni]m}$ is the mean volumetric nitrate uptake rate per aggregate that similar to $Q^m_{[O_2]}$ is obtained through parameterization from pore network model, as explained in the following.

2.2. Parameterization of Nitrate/Oxygen Uptake Rate Functions

A key ingredient for the analytical aggregate model requires input of the mean volumetric uptake rates of oxygen, $Q^m_{[O_2]}$ (respiration), and nitrate, $Q^m_{[Ni]}$ (denitrification). These uptake rate functions are derived from a mechanistic numerical model developed by Ebrahimi and Or (2015) with results parameterized by systematically calculating the resulting microbial consumption rates for a range of aggregate sizes and environmental conditions.

The pore network model describes the emergent life strategies of numerically inoculated individual aerobic and anaerobic microbial cells (e.g., denitrifiers or methanogens in some cases) under quasi-stationary conditions for a set of environmental conditions (e.g., oxygen, carbon, and nitrate contents) and aggregate sizes (in the range of 2 to 10 mm). The resulting rates of oxygen and nitrate uptake were integrated over an aggregate to yield mean volumetric uptake rates that contributed to the parameters used in the analytical model (equations (4) and (5)). It is important to note that the mean uptake rate functions include resource variations, effective transport rates, and microbial cell-level interactions that jointly determine microbial community size and self-organization unique for these specific conditions under consideration (see details in Ebrahimi & Or, 2015, 2016). In the absence of reliable empirical parameters for a wide range of conditions, we rely on mechanistic model parameterization to bridge the gap and provide simple volumetric uptake rate functions as inputs into the analytical aggregate model (for similar conditions as in the detailed model). Fluxes estimated by the analytical aggregate model are then integrated over soil profiles and across landscapes. The model parameters used in the pore network simulations are described in Table S2.

- **Mean Oxygen Uptake Rate Function ($Q^m_{[O_2]}$)**

The numerical results depicted in Figure 2a (see inset) suggest nonlinear relationship between $Q^m_{[O_2]}$ and oxygen content for different aggregate sizes $Q^m_{[O_2]} \propto \sqrt{[O_2]}$. This motivated the normalization of volumetric oxygen uptake rate $Q^m_{[O_2]}$ by (square root of) oxygen concentration, facilitating the plotting of families of normalized $Q^m_{[O_2]}$ as a function of the aggregate size and internal carbon content (Figure 2b). We then fitted a conditional exponential function for the normalized oxygen uptake rate, $\overline{Q^m_{[O_2]}}$ with carbon content ([C]) and aggregate size (R), as given:

$$\begin{cases} \overline{Q^m_{[O_2]}} = \alpha \exp(\beta R), & R > 4\,\text{mm} \\ \begin{cases} \overline{Q^m_{[O_2]}} = \overline{Q^m_{[O_2],R=4}}, & R < 4\,\text{mm} \quad \text{and} \quad [C] < 3\ \text{g/L} \\ \overline{Q^m_{[O_2]}} = c_1 R + c_2, & R < 4\ \text{mm} \quad \text{and} \quad [C] > 3\,\text{g/L} \end{cases} \end{cases} \tag{6}$$

where the fitting parameters (α, β, c_1, and c_2) are obtained from the numerical simulation results, as shown in the inset of Figure 2b for α and β. Recall that we seek to collapse these detailed numerical results of $\overline{Q^m_{[O_2]}}$ for many conditions into simple analytical expressions to be used for the idealized analytical aggregate model.

- **Mean Nitrate Uptake Rate Function ($Q^m_{[Ni]}$)**

The mean value of microbial nitrate uptake rate was quantified for a range of environmental conditions as shown in Figure 3. The numerical results suggest linear relationship between $Q^m_{[Ni]}$ and nitrate concentration ($Q^m_{[Ni]} \propto ([Ni])$). The normalization of $Q^m_{[Ni]}$ demonstrates that the results collapsed to similar ranges of uptake rates for different nitrate concentrations ([Ni]), for given oxygen content and aggregate sizes. We note that the linear relationship is linked to the assumed uniform distribution of nitrate within the aggregate volume and other scenarios of nitrate distribution (similar to the nonlinear relationship between oxygen consumption rate and its concentration along the aggregate) could be used where needed.

For simplicity, and to facilitate simple analytical representation, we fitted power law relationships between nitrate volumetric uptake rates ($Q^m_{[Ni]}$) and aggregate size (guided by the shape of the numerical results). The resulting parameterization of the numerical results is given by a simple analytical expression:

$$\left({}^{Q^m_{[Ni]}} \Big/ _{[Ni]} \right) = \eta \left([O_2]^{-\lambda} \right) \tag{7}$$

where

$$\eta = d_1\left(R^{-d_2}\right)$$

and

$$\begin{cases} \lambda = k_1 + k_2 R, & R < 4 \\ \lambda = e_1\left(R^{-e_2}\right), & R \geq 4 \end{cases} \tag{8}$$

where fitting parameters ($k_{1,2}$ and $e_{1,2}$) are obtained through numerical modeling as shown in the inset in Figure 3.

2.2.1. Effects of Hydration Conditions on GHG Emissions From Individual Aggregates (Hot Spots)

The analytical model proposed by Currie (1962) and Smith (1980) considers a saturated soil aggregate. We extended the model to consider effects of wetting and drying cycles and partially saturated aggregate on the resulting anoxic conditions. For simplicity, aggregate drying was simplified to the transport of vapor diffusing radially from the aggregate into the surrounding unsaturated soil (Haghighi et al., 2013; Shahraeeni & Or, 2012; see supporting information S1 for the details). We divide the aggregate volume into saturated and unsaturated (dry) zones (see inset of Figure S3a). The liquid phase in the saturated region limits gas diffusion whereas the unsaturated shell supports rapid gas diffusion where gas concentration (e.g., oxygen) at the dry shell is in equilibrium with soil air (defined by macroscopic boundary conditions at the aggregate outer surface). Such segregation of the saturated and unsaturated domains enables simple representation of microbial processes in the idealized spherical aggregate, where anoxic conditions occur in the saturated core of the aggregate.

2.3. Biogeochemical Gas Fluxes From a Soil Profile

2.3.1. Soil Biogeochemical Gas Fluxes Form Assemblies of Aggregates

The first step in the upscaling is to integrate biogeochemical gas fluxes over assemblies of aggregates of different sizes located at different depths in a soil profile (hence experiencing different macroscopic boundary conditions). For simplicity, we assume no feedback between members of the aggregate assembly (i.e., the external boundary conditions remain the same for all aggregate sizes) or among aggregate assemblies at different depths in the profile. Many studies have shown that soil aggregate sizes follow a log-normal distribution (Ebrahimi & Or, 2016; Elliott, 1986; Gardner, 1956; Pinheiro et al., 2004). Ebrahimi and Or (2016) have compiled many results showing that for a wide range of measured aggregate sizes (expressed in mm), the log-normal mean parameter (μ) ranges from -2 to 0.2 with a constant log-normal standard deviation of σ = 1. At a given soil depth with similar macroscopic conditions of water, carbon, and oxygen, the total CO_2 and N_2O fluxes are integrated over the log-normally distributed assembly of aggregates according to the process of interest.

For CO_2 flux rates:

$$V_{\text{tot.},CO_2} = \int\int R^3 V_{CO_2}(R) f(R) \mathrm{d}R / \int R^3 f(R) \mathrm{d}R \tag{9a}$$

For denitrification-produced nitrous oxide rates:

$$V_{\text{tot.},N_2O} = \int\int R^3 V_{N_2O}(R) f(R) \mathrm{d}R / \int R^3 f(R) \mathrm{d}R \tag{9b}$$

where $f(R)$ is the log-normal distributions of aggregates of different size classes, parameterized through field observations (Ebrahimi & Or, 2016). It should be noted that $V_{\text{tot.}}$ only accounts for gas fluxes from assembly of hot spots, and the contribution of soil matrix is added when upscaling to soil profile (see section 2.3), while their contribution becomes negligible at dry conditions.

The contribution of bulk soil (the nonaggregated soil volume at each layer) to GHG emissions is added to the fluxes from aggregates. We assume that each soil layer in the profile contains a similar fraction of aggregates (amount here to 0.3 of the soil volume). The bulk fraction of a soil layer is uniform with respect to water, oxygen, and carbon contents. Hence, GHG production rate within bulk soil is calculated from mean nitrate and oxygen uptake rates (Q_m) with respect to the respective substrate contents at a given depth. We note that the distribution of hot spots represented by hypothetical aggregate size distribution derived from agricultural soils is probably the weakest ingredient in this model approach. Hot spots in carbon-rich arctic soils would probably form many different mechanisms and may be distributed differently; nevertheless, the exact distribution does not affect the upscaling scheme proposed in this study. A critical lack of methods and direct

observations of hot spots hampers advances in mechanistic modeling as proposed in this study. Insights from manipulative experiments as reported in Ebrahimi and Or (2018) advance our understanding concerning the role of carbon distribution in soil aggregates on GHG emissions; yet, methods for field characterization of hot spot distribution are essential for linking detailed mechanistic with large-scale models (as required for ESM).

2.3.2. Profile-Scale Representation of GHG Fluxes and Boundary Conditions

The natural distributions of ambient conditions (e.g., temperature and moisture) and resources (e.g., carbon and oxygen) over a soil profile (as schematically depicted in Figure 1) vary across the landscape and affects microbial community dynamics and function (Fierer et al., 2003, 2009; Tecon & Or, 2017). We coupled the assumed vertical distributions of resources (carbon and oxygen) and conditions (water content, temperature) with the aggregate biophysical model to address spatial variations in microbial processes that give rise to activity in hot spots from which much of the soil GHGs emanate (Davidson et al., 1998; Groffman et al., 2009; Kuzyakov & Blagodatskaya, 2015).

To upscale the biogeochemical gas production rates from an assembly of soil aggregates, and their emission from a soil surface, we employed a scheme from Ebrahimi and Or (2016). The soil profile is discretized to layers of thickness (Δz), each layer containing aggregates of different sizes, and the prevailing conditions at that layer serve as similar macroscopic boundary conditions for all aggregates. To reduce the computational burden for large-scale applications, we consider three soil layers only (see Figure S2). The macroscopic variations in abiotic factors and resources are provided as input parameters for the analytical aggregate model solved for each soil layer. The spatial and temporal variations in macroscopic boundary conditions are discussed in detail by Ebrahimi and Or (2016), and here, a brief description on water and oxygen profiles over the soil depth is provided in the supporting information.

The primary transport mechanism for GHG in the soil is diffusion through the liquid phase in the saturated zone of the soil profile (or the saturated core of an aggregate) and through the gas phase in soil pores in the unsaturated (aerated) zone. For the aerated zone of the soil profile, we assume that the gas concentrations in soil water and soil air are in the equilibrium according to Henry's law. With such an assumption and given the relatively high gas diffusion compared to liquid phase, gas productions from the aerated fraction of the soil profile is assumed to be directly emitted at the soil surface without accumulation in the profile. In contrast, microbial gas production in inundated soil layers in the profile may accumulate due to the slow diffusion rates through the liquid phase.

To estimate the net GHG diffusive flux within saturated zone of the soil profile, a diffusion-reaction equation over the soil depth is solved (Ebrahimi & Or, 2017):

$$\left(J^{d+1}_{\text{tot,liq.}}\right) + Q_{\text{acc.}} = \left(J^{d-1}_{\text{tot,liq.}}\right) + S_{\text{d,diff.}} \tag{10}$$

where $Q_{\text{acc.}} = \Delta z\left(\frac{A_{\text{liq.}}\Delta C_{\text{liq.}}}{\Delta t}\right)$ is the flux accumulation term within the layer d. $C_{\text{liq.}}$ is the gas concentration in liquid phase within the corresponding soil layer. $S_{\text{d, diff.}}$ is the total gas production rate from aggregate assemblies and the bulk fraction of the soil layer, calculated with respect to soil profile aggregate fraction, $f_{\text{agg.}}$.

$$S_{\text{d,diff.}} = f_{\text{agg.}}(V_{\text{ass.}}) + \left(1 - f_{\text{agg.}}\right)V_{\text{bulk}} \tag{11}$$

$V_{\text{ass.}}$ is the volumetric CO_2 or N_2O production rates from the assembly of aggregates obtained from equations (9a) or (9b), respectively. V_{bulk} is the volumetric GHG production rate from bulk soil. Additionally, the gas flux from the aerated portion of the soil profile is directly obtained through superpositioning of GHG production rates in equations (9a) and (9b).

3. Large-Scale Temporal and Spatial Variations in Soil GHG Emissions

Many of the soil GHG quantification techniques either rely on closed chamber measurements with a small footprint (less than 1 m^2) that underrepresents soil spatial variations or employ eddy covariance flux measurements with extensive mixing of spatially variable sources within the measurement footprint. Keeping these two scenarios in mind, we seek to derive regional GHG fluxes by systematically upscaling fluxes from representative soil profiles for the landscape of interest. For illustration purposes, we evaluate the proposed upscaling strategy over spatiotemporal scales where model predictions for N_2O emission rates are compared with measured emissions from ecosystems experiencing seasonal variations in water content and temperature. We focus on N_2O fluxes; however, other soil GHGs could be considered within the same

upscaling framework, as illustrated in a recent study of seasonal methane emissions from a thawing permafrost soil (Ebrahimi & Or, 2017).

We applied an analytical model to seasonal variations in soil N_2O emissions for two case studies of minerotrophic fens. Case study I is located at central Finland (part of Lakkasuo mire complex; Martikainen et al., 1993) where the region was partially drained for forestry (case study I), and case study II is located in northeastern Bavaria, Germany, where rainfall intercepted on the surface was manipulated using rainfall shelters (Goldberg et al., 2010). In these two case studies, water table fluctuations and rainfall patterns altered saturation conditions and thus affected GHG emission dynamics. GHG emissions from the northern peatlands (case study I) were deemed particularly important because these peatlands store 20% to 30% of the Earth's organic nitrogen (Gorham, 1991; Martikainen et al., 1993). Additionally, the model is applied to quantify spatially heterogeneous N_2O emissions at regional scale for a subarctic field located in Northeast European Russia, Seida (Voigt et al., 2016; case study III). Recently, the region is experiencing permafrost warming and thawing that provides important case studies for impacts of climate change on similar systems (Oberman & Mazhitova, 2001; Romanovsky et al., 2010; Voigt et al., 2016). For case study III, the mean annual temperature and precipitation in the region are −5.8 °C and 505 mm, respectively (Repo et al., 2009). The region is composed of various land cover classes such as tundra, peatland, forest, and willow groves (Hugelius et al., 2011a).

- **Seasonal Variations: Thermal and Hydrologic Dynamics**

The dynamics of soil water content profiles are affected by hydrological processes that remove (e.g., root water uptake, evapotranspiration, and drainage) or add (e.g., precipitation and permafrost thaw) water to the soil. For simplicity, we do not solve explicitly the hydrologic dynamics of well-established hydrological models (Clark et al., 2015; Simunek et al., 2012) and provide the water content profiles as inputs (extracted from observations or assumed). For the case studies I and II, information on water table variations is available at daily time intervals, and hydrostatic conditions for the water content profile above the water table are assumed (Ebrahimi & Or, 2016). For case study III, where water table depths are not provided (Voigt et al., 2016), we carry out a simple water balance using field data on daily evaporation and precipitation rates (details of model formations are provided in supporting information S2).

To represent the temperature dependency of nitrate and oxygen uptake rates at seasonal scales, we applied the widely used Q_{10} index that considers proportional changes in production rate given a 10 °C change of temperature. The uptake rate (Q^m) could be then related to temperature as given:

$$Q^m = Q^m_{25} \exp\left(\beta'(T-25)\right) \tag{12}$$

where Q^m_{25} is the oxygen or nitrate uptake rate at 25 °C. β' is related to Q_{10} value ($Q_{10} = \exp(10\beta')$). Q_{10} values used in this study are provided in Table S2. Note that we used constant Q_{10} values, but more studies are required to quantify its variation ranges and sensitivity to temperature and ecosystem characteristics (Davidson et al., 2006; Schipper et al., 2014; Wang et al., 2014).

In addition to temporal changes, spatial heterogeneities in the site characteristics (e.g., soil texture, landscape slopes, and permafrost presence/absence), land cover, and chemical properties (e.g., OM content, pH, and C:N ratio) of an ecosystem may significantly affect the resulting spatial patterns of GHG emissions (Repo et al., 2009; Scott-Denton et al., 2003; Tang & Baldocchi, 2005; Townsend et al., 2008; Zona et al., 2016). To incorporate spatial heterogeneities, we use satellite land-cover imagery to characterize soil classes and biomes. We then base the upscaling strategy on a detailed map of a landscape from a fragmented permafrost zone in Northeast European Russia, Seida (67°03′N, 62°55′E; Voigt et al., 2016; Figure 4). A map of selected chemical and physical properties (bulk density, C:N ratio, and respiration) of each of the biomes in the landscape was constructed over a grid (each grid point was treated as a soil profile, no lateral interactions among profiles). We used ranked correlated surfaces to visualize the synthetic maps for visualization purposes (Schrenk et al., 2012). The chemical and physical properties including organic matter content, respiration rate, C:N ratios, and bulk density were extracted from literature data on field measurements (Gil et al., 2017; Repo et al., 2009; Voigt et al., 2016) and mapped as shown in Table S1 (and Figure S5 for respiration rates from different ecosystems). The upscaled biophysical model is linked to hydrologic and thermal modules to estimate soil water content and temperature profiles (see supporting information Figure S2 and Ebrahimi & Or, 2017). The hydraulic model parameters for large-scale applications could be obtained either from field observations

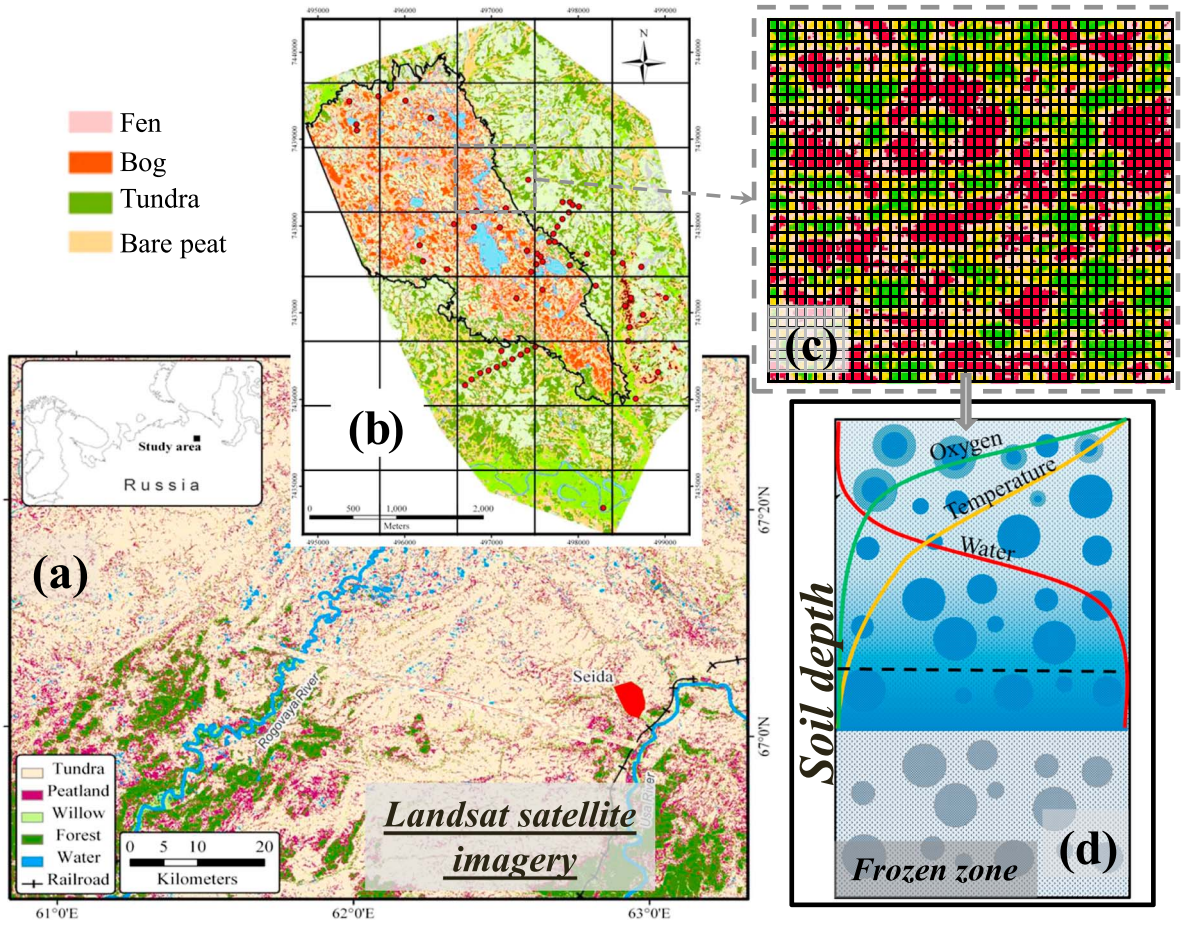

Figure 4. Representation of the upscaling strategy of biophysical analytical model from soil profile to regional scale. (a) Map of the geographical location of case study III used for modeling spatial variations in GHG emissions with generalized land-cover extracted from Landsat satellite imagery. (b) Land cover classifications based on Quickbird satellite images (2.4 m pixel size). The images are modified after Hugelius et al. (2011a). For detailed description of the land-cover classification techniques, see Repo et al. (2009) and Hugelius et al. (2011b). (c) Synthetic map representing chemical and physical properties of study site in mesh grid, each grid representing a soil profile (d).

or from hydraulic pedo-transfer functions (Tóth et al., 2015). Additionally, readily available soil global maps at high resolution (e.g., *soilgrids*; Hengl et al., 2017) could be used to extract soil physical and chemical properties for the region of the interest.

The biogeochemical gas fluxes, produced over each grid cell ($j_{p.}$) or soil profile, were integrated by the superpositioning of fluxes over the landscape yielding regional estimates of GHG emission rates from the soil surface:

$$J_{tot.} = \sum_m \sum_n j_{p.}([C], [C:N], BD, ER, \theta_{surf}, T_{surf}) \quad (13)$$

The analytical model at regional scale requires information on carbon content [C], C:N ratios, bulk density (BD), respiration (ER, modifying $w_{[O_2],0}$ in equation (A9) in the supporting information for oxygen profile), and temporal variations in soil surface water content (θ_{surf}) and temperature (T_{surf}) to provide reliable predictions of GHG fluxes.

4. Results and Discussions

4.1. Effects of Aggregate Size and Hydration Conditions on Sizes of Anoxic Microsites

We first illustrate some of the important features of the analytical model for estimating biogeochemical fluxes from individual aggregates. The size and activity within anoxic zones formed in individual aggregates and the

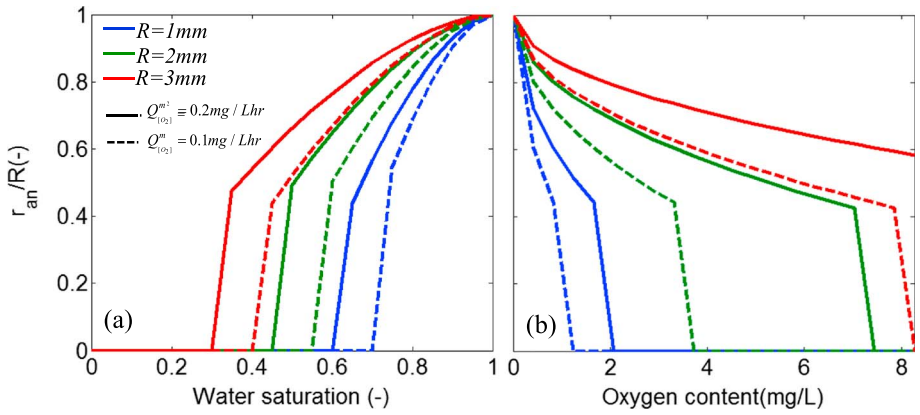

Figure 5. Analytical aggregate model predictions for the size of the anoxic regions (scaled by aggregate size *R*) with changes in (a) water saturation (constant oxygen content at boundary, 0.5 mg/L) and (b) oxygen concentration at the aggregate surface (with constant water saturation, 0.7). Simulations were conducted for three aggregate sizes and two mean volumetric oxygen uptake rates. The anoxic zone is defined as the radius of the aggregate where the oxygen consumption rate becomes zero.

production rates of GHG (N_2O and CH_4) are determined primarily by the aggregate size (diffusion length), saturation level (diffusion rate), and oxygen consumption rate (Ebrahimi & Or, 2015; Tiedje et al., 1984). Simulation results, in Figure 5, summarize the effects of water saturation and oxygen content (i.e., determined by location in the soil profile) on the sizes of anoxic zones within aggregates of different sizes for two values of volumetric oxygen uptake rates per aggregate (microbial activity levels). The results in Figure 5a show that with increasing water saturation or reducing the oxygen content at the aggregate surface, the size of the anoxic zone expands. Considering, for example, aggregates of 1 mm in radius, no anoxic zone would form until saturation reaches 0.6 or oxygen content in the bulk soil air (or at the aggregate surface) drops to values smaller than 2 mg O_2/L. These results are consistent with detailed modeling and observations that also support the importance of aggregate size in determining the resulting anoxic zone size (Ebrahimi & Or, 2016; Horn et al., 1994).

4.2. Seasonal Variations of GHG Emission Rates and Patterns: Model Upscaling

For model evaluation, we simulated the seasonal variations in soil N_2O emissions for case studies I and II where variations in soil temperature and water table levels were provided as inputs as seen in Figures 6b and 6c, respectively (peat soil properties are represented in Table S1). The biophysical analytical model estimated seasonal patterns of N_2O emissions in reasonable agreement with field observations (Figure 6a). In a recent laboratory experimental study (Ebrahimi & Or, 2018), we observed that changes in water table position within a soil column exerted strong and rapid influences on N_2O emission rates within a day. We conjecture that such short-term effects may have been averaged out in the coarse field observations (measured one to four times a month), yet such short-term dynamics were preserved in the model simulations. The mechanistic model captures features of the late season N_2O fluxes observed in the field data. The model results indicate that N_2O emissions during the summer (with high temperature/aerated conditions) were governed by N_2O production from the largely aerated zones in the soil profile (that contain saturated aggregates/hot spots). In contrast, cold-season N_2O emissions seem to be dominated by diffusion from the inundated (saturated) portions of the profile where N_2O production slowly becomes limited by low temperatures (see Figure S4) until it ceases upon freezing.

In addition to water table fluctuations, the rainfall patterns during the summer contribute to enhancement of N_2O emissions from waterlogged peat soils (especially during dry periods). Such surfaces have been previously overlooked as marginal sources of N_2O emissions (Augustin et al., 1998; Goldberg et al., 2010; Martikainen et al., 1993; Regina et al., 1996). To evaluate the effects of rainfall patterns, in the second case study, we applied the modeling approach to estimation of N_2O emissions from fen soil during summer time with low rainfall and soil evaporation (Goldberg et al., 2010). The experimental field in the second case study experiences mean annual temperature of +5.3 °C and the mean annual precipitation of 1,160 mm that imparted relatively wet conditions throughout the year (Goldberg et al., 2010).

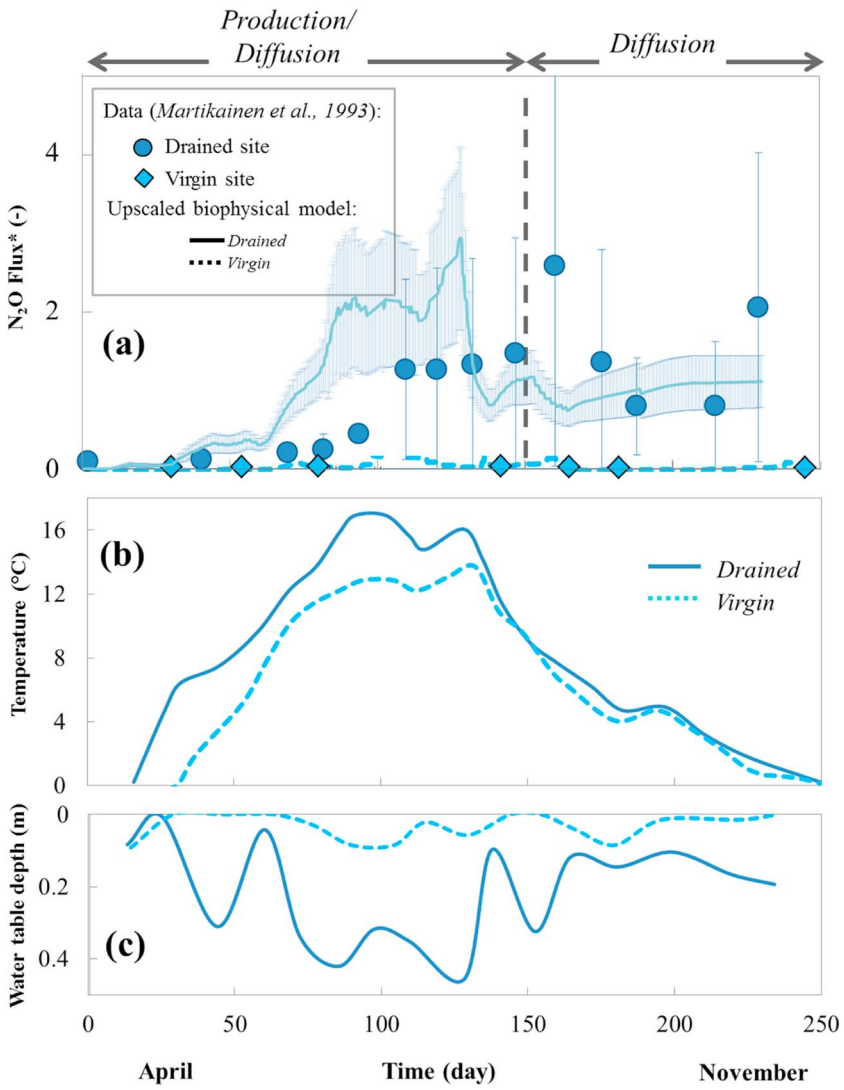

Figure 6. Case study I: (a) Normalized daily N_2O emissions from field observations compared with simulations for soil profiles. The field data are shown with symbols, and simulation results are indicated with solid and dashed lines for drained and virgin soils, respectively. Black dashed lines separate time zones with diffusive dominant flux from time period with highest production and emission from aerated fraction of soil profile. (b) Seasonal variations of temperature and (c) evolution of water table depth as a function of time for two field case studies (drained versus virgin). Lines in (b) and (c) indicate the linear interpolations of field data (symbols) used as input for simulations. The N_2O emission rates are normalized with averaged emission rates for sake of comparison. The averaged emission rates of drained site for field data was 38.6 μg (N_2O) m^2/hr and for the simulations were 1.02 μg (N_2O) m^2/hr. The mean aggregate size of 2 mm is considered for simulations.

Model simulations for seasonally varying water table levels and air temperatures for case study II (shown in Figure 7) were compared with N_2O emissions from plots that were sheltered from rainfall (Goldberg et al., 2010). The key parameters used in the simulations for the fen soil are presented in Table S3. Simulation results were generally consistent with field observations, showing low N_2O emissions from water-logged soils, whereas the sheltering of soil surface from rainfall during periods of high evaporation resulted in considerable N_2O surface fluxes (Figure 7).

These model results confirm previous experimental observations that attribute soil N_2O production to microbial denitrification in anaerobic anoxic hot spots (Davidson, 1991; Goldberg et al., 2010). The modeling results here, guided by experimental and numerical analyses (Ebrahimi & Or, 2018), highlight the importance of anoxic hot spots and their size distributions within the soil unsaturated zone as potentially important

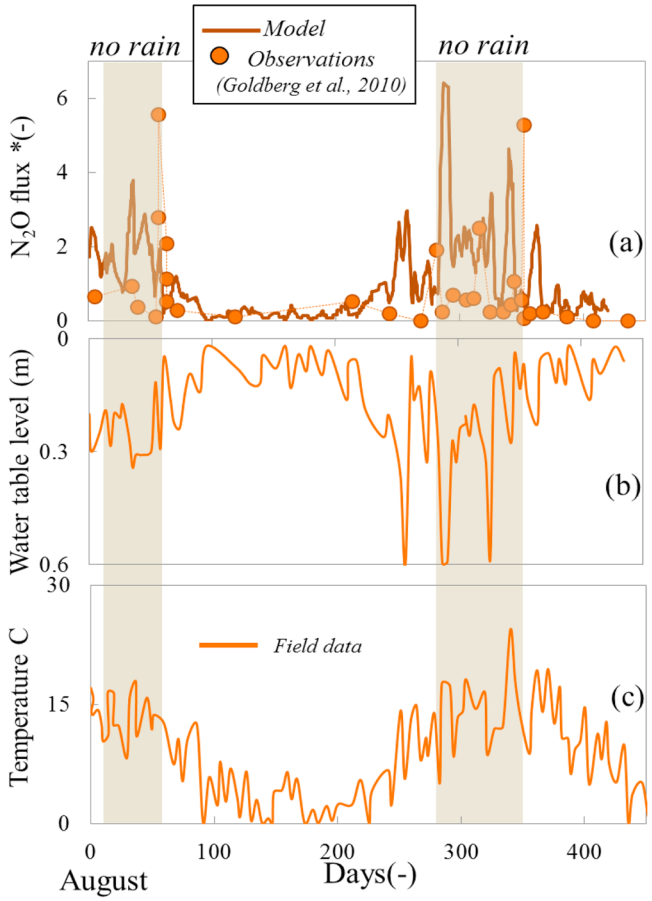

Figure 7. Case study II: Effects of summer no-rain period on N_2O emission rate. (a) Daily N_2O emissions from field observations compared to simulations. (b) Seasonal variations of water table level and (c) evolution of air mean daily temperature as a function of time extracted from field data (Goldberg et al., 2010). The field data are shown with symbols, and simulation results are indicated with solid lines. The N_2O emission rates are normalized with averaged emission rates for sake of comparison where the averaged emission rates for field data was 282.9 μg (N_2O) m^2/hr and for the simulations were 37.4 μg (N_2O) m^2/hr. No-rain events are experimentally made in the field study by a roof and by extracting groundwater from drainage tiles (Goldberg et al., 2010).

sources of N_2O emissions (denitrification is promoted exclusively in the hot spots where oxygen levels are low). Note that under unsaturated conditions, the dominance of gas diffusion removes N_2O emitted from the aggregated via the soil gas phase, thereby preventing the complete denitrification pathway from N_2O to N_2 that would have occurred in saturated soil (inundated portion of a soil profile).

Considering the importance of water table level fluctuations as also predicted for climate change scenarios (Goldberg et al., 2010; House et al., 2016; Taylor et al., 2013), the incorporation of such fluctuations and drier conditions (reduced rainfall events) are important aspects for more reliable predictions of future GHG emissions and budgets (Ebrahimi & Or, 2018; Liengaard et al., 2012; Markfoged et al., 2011; McClain et al., 2003). Consistent with previous experimental study (Ebrahimi & Or, 2018), our modeling results in Figure 6 indicate that the duration and intensity of anoxic conditions play an important role in the dynamics and intensity of N_2O production. The observed N_2O flux may be enhanced under moderate wetting events (drained scenario in Figure 6 where aggregates are wet but gas diffusion rates allowed through the unsaturated interaggregate porosity remains high). In contrast, no N_2O emissions were observed under intense wetting events (virgin scenario in Figure 6: flooded soil) due to suppressed diffusion and escape from the aggregate. Remarkably, such flooding events promote the direct conversion of N_2O to N_2 before emission of N_2O from soil can take place (more details are found in Ebrahimi & Or, 2018, regarding "hot moments" for N_2O emissions). Such dependency of microbial production of N_2O to duration and intensity of anoxic conditions are taken into account in current simple quasi-stationary hydrology model by explicit coupling of gas diffusion and storage within the soil profile. A comprehensive hydrology model would be necessary to accountably account for water table dynamics at large scales that may include rapid changes in the landscape that is beyond the scope of this study (Liljedahl et al., 2016; Pomeroy et al., 2007).

4.3. Regional-Scale Spatial Variations in GHG Emissions

Building on the promising results of the upscaled biophysical-analytical model presented in the previous sections, we seek to study effects of landscape-scale spatial heterogeneity such as soil texture, resource distribution, and water table dynamics on regional soil GHG emissions. Although the existence of spatial variations in GHG emissions due to patterns of abiotic factors are well known and acknowledged, their incorporation in process-based models remains limited to calibration of field observations (He et al., 2014; Manzoni et al., 2016; Wieder et al., 2015).

The analytical biophysical model was applied for the detailed distribution maps of chemical and physical properties for the case study III located in Northeast European Russia, Seida (Voigt et al., 2016). For simplicity, we focus on modeling N_2O emissions from a complex landscape that is part of the permafrost plateau, a surface composed of upland tundra, bog, fen, and bare peat (Gil et al., 2017). A detailed classification of the land cover based on Landsat (30-m pixel sized multispectral image) and Quickbird (2.4-m pixel sized multispectral image) imagery are described by Hugelius et al. (2011b) and shown in Figure 4.

The working hypothesis is that the large spatial heterogeneities within a few kilometers would give rise to local hot spots for N_2O production at scales larger than aggregates (m^2 to km^2) due to local hydrology, as has been observed in field studies (Gil et al., 2017; Repo et al., 2009; Voigt et al., 2016). For example, bare peat (also called "peat circles"), representing only 5–10% of the peat plateau landscape, has been shown to emit

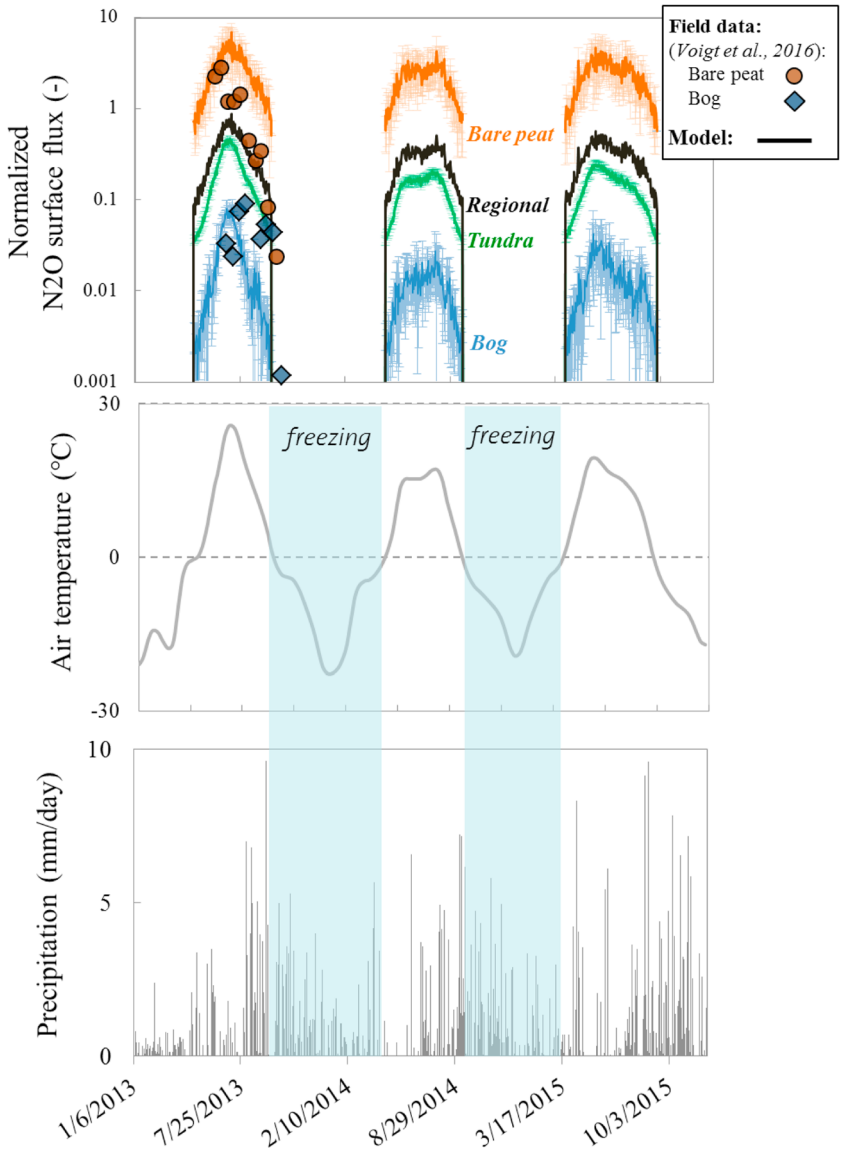

Figure 8. Case study III: Effects of spatial heterogeneity on N_2O fluxes. (a) Seasonal variations for N_2O emissions for three consecutive years in comparison with field observations where available. (b) Seasonal variations of air temperature. (c) Daily precipitation rates, obtained from station data of closed city to field observations, Abez (database: World Meteorological Organization and www.worldweatheronline.com). The field data are shown with symbols, and simulation results are indicated with solid lines. The N_2O emission rates are normalized with averaged emission rates from bare peat. The N_2O emission rates are normalized with averaged emission rates of emissions from bare peat for sake of comparison where the averaged emission rate for field data was 35.65 μg (N_2O) m^2/hr and for the simulations was 4.71 μg (N_2O) m^2/hr.

N_2O at rates are as high as emissions from agricultural or tropical soil (Elberling et al., 2010; Gil et al., 2017; Marushchak et al., 2011; Repo et al., 2009). We simulated seasonal variations in N_2O fluxes for three consecutive years using regional temperature and precipitation data from the closest station *Abez* as input (Figure 8). The modeling study uses field data for precipitation and air temperature measurements from 2013 to 2015 growing seasons and subsequent freeze-in periods (Huffman et al., 2016), as shown in Figures 8b and 8c.

The model results of seasonal N_2O fluxes form individual land covers (represented as typical soil profiles for each cover) are shown in Figure 8a. The modeling results are consistent with the small number of field observations that depict high N_2O emissions from bare peat relative to other ecosystem types (i.e., fen, bog, and tundra). The model captures effects of seasonal temperature variations, consistent with the field

observations of (Gil et al., 2017; Marushchak et al., 2011; Repo et al., 2009; Voigt et al., 2016). Unlike the case study II, depicted in Figure 7, the subarctic region studied here exhibited relatively stable water table level throughout the summer season due to high number of rainfall events and low evaporation; hence, we observe fewer saturation-induced variations in N_2O emissions during the season. The model considers potential climate change scenarios and resulted variations in regional hydrology (flooding and droughts) that, in turn, could affect N_2O emissions and budgets, as studied in Figure 8 and predicted by current hydrological models (Goldberg et al., 2010; House et al., 2016; Taylor et al., 2013).

The importance of detailed spatial heterogeneities on regional-scale fluxes could be assessed from regional-scale N_2O fluxes for case study III depicted in Figure 8. We have studied how N_2O emissions vary during wet and dry (saturated aggregates in an aerated bulk soil) scenarios under quasi-stationary conditions as depicted in Figure 9. The local variations in respiration (considering plant and microbial processes) and C:N ratios are spatially distributed over a synthetic map of land cover as shown in Figure 9b. The field data for the range of C:N ratios are obtained from Repo et al. (2009), and the distribution of mean respiration rates are shown in Figure S5 extracted from field observations (Voigt et al., 2016).

The results highlight the importance of spatial heterogeneities in physical and chemical properties of an ecosystem and interactions with hydrology that may give rise to formation of hot spots for GHG production. For example, the bare peat covers only about 10% of the Seida region, yet emissions from that ecosystem accounts for more than 50% of the regional N_2O flux, a result consistent with field observations (see Figure 9 and the mean seasonal N_2O emission at regional scale in Figure 8). Additionally, model results suggest that changes in soil water content affect N_2O fluxes differently in different ecosystems. For example, N_2O emissions were highest from peatland (especially bare peat) under wet conditions but significantly drop under aerated and dry conditions. In contrast, N_2O emissions from Tundra were maximized under dry conditions and suppressed under the wet scenario. These differences are attributed to the spatial variations in net respiration rates (shown in Figure 9a) that affect the oxygen content profiles in the soil as described by equation (A9) in the supporting information. For these synthetic case studies, higher respiration rates over Tundra regions induce highly anoxic conditions under wet scenarios that favor complete denitrification (from N_2O to N_2), whereas low respiration of bare peat provides conditions that promote anaerobic activity while preserving sufficient oxygen to prevent complete denitrification.

The present modeling approach highlights the important effect of respiration on denitrification where respiration rate may modify the soil oxygen profile with soil depth. More studies are needed to quantify and incorporate such feedback (in process based models) and to elaborate seasonal effects of respiration and chemical properties of the soil profile on N_2O production. Additionally, the model was capable of capturing effects of hydrothermal seasonal dynamics at the regional scale (soil temperature variations) as seasonal hydrothermal patterns may improve predictions of N_2O emission dynamics. For example, global warming is projected to increase rainfall intensity (Kunkel et al., 2013; Trenberth, 2011), and such events have been traditionally assumed to enhance N_2O emission rates (Butterbach-Bahl et al., 2013; Griffis et al., 2017), but explicit consideration of intensity and duration of wetting/evaporation processes shown in this study challenge this notion.

Unlike the mechanistic modeling approach presented here, empirical first-order models often represent microbial activity by assuming biological homogeneity and functional equivalence and consider microbial response for environmental changes to be invariant across ecosystem and through temporal scales (Bradford & Fierer, 2012; Wieder et al., 2015). Without considerable level of local tuning, the predictive capabilities of such models would be questionable especially for estimation of fluxes for different spatiotemporal and climatic conditions (Baldocchi, 2014; Hawkes & Keitt, 2015; Manzoni & Porporato, 2009; Wieder et al., 2015).

4.4. Uncertainties and Future Directions

In the current model, a daily quasi-stationary condition is considered that neglect the time delay between production within the aggregates and emission of GHG from aggregate surface. More studies are required to address the temporal accumulation of biomass and products within the aggregates that will affect emission dynamics as has been observed in previous soil column scale experiments (Ebrahimi & Or, 2018; Rabot et al., 2015). Additionally, input data from field observations (e.g., temperature and respiration) for seasonal

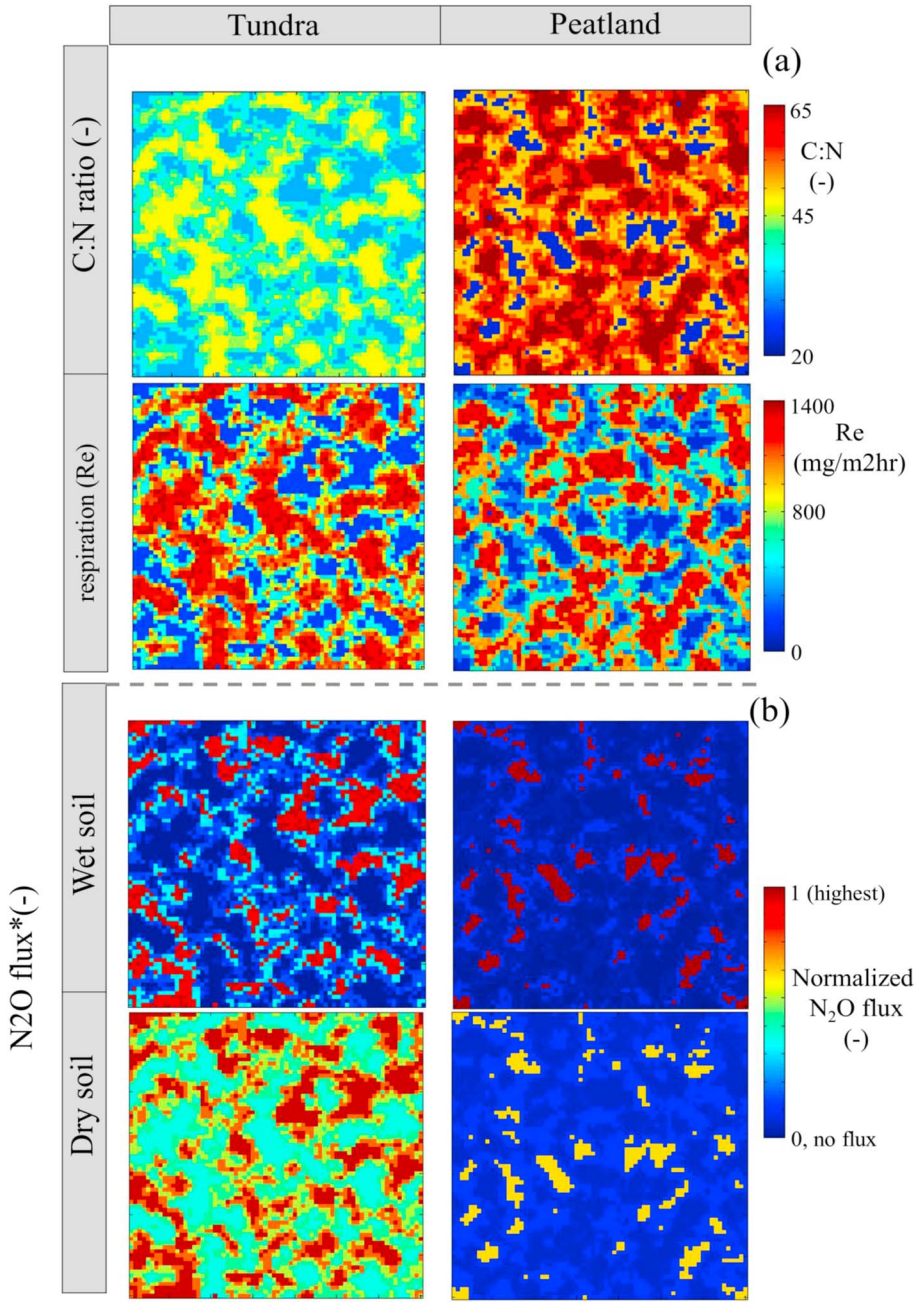

Figure 9. N_2O flux from synthetic scenarios of land cover (tundra and peatland) from study site, Seida, Russia. (a) Spatial heterogeneities in C:N ratio and respiration, as extracted from field observations (Repo et al., 2009; Voigt et al., 2016). (b) Spatial variations in local N_2O fluxes of study regions for wet and dry (aerated) conditions under quasi-stationery conditions. The fluxes are normalized based on maximum N_2O fluxes from each ecosystem (peatland: 65.92 and tundra: 9.46 μg (N_2O) m^2/hr).

dynamics of GHG emissions have been used as daily averaged data and thus neglect important diurnal effects that has been shown to impact GHG emissions (Nishimura et al., 2015; Shurpali et al., 2016).

The current study takes preliminary steps toward linking field observations and attempts to parameterize large-scale biogeochemical gas flux models with measurable quantities. The model accounts for soil GHG emissions for certain scenarios of carbon pools within soil aggregates ("hot spots") that may be consumed by aerobic and anaerobic microbial communities. The background gas fluxes due to microbial activity in the soil matrix and its variation with hydration, temperature, and carbon content is added to

biogeochemical fluxes from soil aggregates. The full representation of ecosystem level carbon balances and dynamics (Foley et al., 1996; Sitch et al., 2008), as done in Earth system models, requires more complete account of various carbon inputs (e.g., litter decomposition and root exudates) and outputs (reparation and discharge) and well beyond the scope of this mechanistic study. The current model advances capabilities to systematically evaluate the roles of various distributions and concentrations of carbon sources in soil that combined with novel experimental techniques allow testing soil structural effects and nutrient landscapes on microbial processes especially in the context of soil carbon hot spots (i.e., aggregates). The inclusion of mechanistic aspects of microscale processes within a regional-scale soil GHG emissions (with certain upscaling assumptions) could in a "coarser" form contribute to the strengthening of Earth system models by improved process description. More observations are required to provide insights on microbial community dynamics (e.g., methanogens, denitrifiers, and ammonia oxidizers) as abiotic factors change (e.g., temperature, water content, oxygen level, C:N ratio, pH, NH_4^+, and nitrate) to refine the current model (Graham et al., 2012; Jansson & Taş, 2014). Additionally, more studies are required to investigate the significance of aerobic nitrification and its role on increasing nitrate concentration, as necessary substrate for denitrification pathway (Regina et al., 1996; Robertson & tiedje, 1987).

Advanced experimental techniques (e.g., X-ray imaging) should be applied to characterize structural heterogeneities of subarctic organic soil texture (e.g., bulk density, aggregate fraction, and pore space properties) and their hydrological properties that will significantly reduce uncertainties associated with the model predictions (Schweizer et al., 2018; Totsche et al., 2018), as also analyzed by Ebrahimi and Or (2018). For instance, pore-scale modeling has revealed that methane emission rate from bulk soil significantly differs from aggregates that highlights the importance of considering such structural hot spots (Ebrahimi & Or, 2017). Additionally, the mean pore size and aggregate size distributions substantially influence substrate and oxygen diffusion rates and thus regulating the dynamics of aerobic and anaerobic microbial communities that changes GHG fluxes (Ebrahimi & Or, 2015, 2016; Horn et al., 1994).

The parameterization of GHG productions from the current pore-scale model has been performed by assuming that the growth kinetic properties are driven from isolated cultures of batch experiments where only a single dissolved substrate (e.g., glucose) is considered (Table S2). Experimental studies are needed to quantify growth kinetics in response to the environmental conditions (e.g., variations in pH and chemical components) that microbial communities experience in the corresponding ecosystem. Most importantly, the growth kinetics from dissolved substrate neglects the enzymatic activity necessary to break down particulate organic matter that could lead to overestimation of the actual kinetic rates (Drake et al., 2013; Manzoni et al., 2012).

5. Summary and Conclusions

The proposed analytical framework addresses a longstanding challenge of mechanistic representation of microbial functioning and response to variations in soil and ambient conditions on biogeochemical fluxes across scales ranging from aggregates to landscapes. The mechanistic modeling approach departs from traditional approaches that rely on heuristically linking pools of organic matter with microbial biomass (Manzoni et al., 2014) or adapting Michaelis-Menten parameters to capture microbial dynamics and spatial variations (Wieder et al., 2014). The biophysical model proposed in this study explicitly accounts for soil structural elements (aggregates as hot spots for microbial life) and could provide guidance for future biogeochemical process-based model and data gathering from field observations.

The analytical model represents soil aggregates as idealized spheres in which substrate diffusion and consumption processes vary radially. A key step in the model development was the parameterization of microbial activity functions based on systematic evaluation of detailed individual microbial life in a pore network mimicking an aggregate (Ebrahimi & Or, 2015). This parameterization bridges a major gap due to the lack of experimental information and a prohibitively costly pore-scale model of microbial life for landscape-scale modeling. We have systematically varied ambient conditions, aggregate sizes, and derived from the results of the detailed model functions for quantifying mean uptake rates of oxygen and nitrate per aggregates. These functions are the closest representation we have to consideration of microbial community self-organization and composition in response to changes in the environmental conditions (e.g., carbon, oxygen, and nitrate contents).

The analytical model was upscaled to provide estimates of spatial and temporal variations in N_2O emission rates for two case studies from peatland and fen fields. The model evaluates N_2O emission dynamics in response to water table fluctuations and seasonal changes in the temperature, in comparison with field observations. Additionally, the model captures the effects of temporally reduced rainfall events to enhance N_2O emissions, consistent with field observations.

Current modeling strategy systematically captures the dominant role of spatial heterogeneities from small (e.g., aggregates) to landscape (e.g., bare peat in present study) scales that gives rise to creation of temporal hot spots for GHG productions in agreement with limited observations.

Clearly, the strategy of using results from a detailed pore-scale model with local microbial interactions to parameterize an analytical and upscalable model is merely a compromise to overcome information (lack of experimental parameters) and scale gaps. The implementation of such cascade of models at different levels of process representation requires a more rigorous validation, and thus, the results remain tentative. The results suggest that more studies are required to systematically evaluate emergence of large-scale hot spots in certain environments (e.g., intense fluctuations and droughts) that would dominate regional-scale fluxes. The study provides a means for using high-resolution satellite imagery to integrate land-cover attributes with physical and chemical properties of rapidly changing environments such as Polar Regions.

The major challenge to incorporate such mechanistic approach for large-scale applications is still characterizing the hot spot size distributions with measurable quantities (Abramoff et al., 2018). Representation of aggregates as structural element for soil biological hot spots is first reasonable approximations, but further characterizations are necessary to identify variability of these hot spots. In the absence of measurement techniques, the current model could potentially be combined with field observations on net GHG emissions and their dynamics to optimize hot spot size distributions through inverse modeling techniques.

The major challenge for the incorporation of the mechanistic approach proposed here for large-scale applications remains the characterization of the nature of hot spots and their size distributions based on simple-to-measure methods (Abramoff et al., 2018). The approach we have taken of using aggregates as ubiquitous structural elements that result from soil biological hot spots represents an approximation of a broader range of hot spots in different soil systems (natural and managed). In the absence of direct measurements of hot spots, we envision the use of the current model combined with field observations of GHG emissions and their dynamics as a means for identification of probable hot spot size distributions through inverse modeling (Davidson et al., 2014).

Acknowledgments
The financial support of the European Research Council (ERC) Advanced Grant (320499—*SoilLife*) and by SystemsX.ch (*MicroScapesX* project) are gratefully acknowledged. A. E. acknowledges funding from the Swiss National Science Foundation (SNSF grant P2EZP2_175128) during his stay at MIT. Mathematical code supporting the obtained results is available in GitHub repository (https://github.com/aliebmit-edu/SoilFlux-version-1.xx).

References

Abramoff, R., Xu, X., Hartman, M., O'Brien, S., Feng, W., Davidson, E., et al. (2018). The millennial model: In search of measurable pools and transformations for modeling soil carbon in the new century. *Biogeochemistry*, *137*(1-2), 51–71. https://doi.org/10.1007/s10533-017-0409-7

Ananyeva, K., Wang, W., Smucker, A. J. M., Rivers, M. L., & Kravchenko, A. N. (2013). Can intra-aggregate pore structures affect the aggregate's effectiveness in protecting carbon? *Soil Biology and Biochemistry*, *57*, 868–875. https://doi.org/10.1016/j.soilbio.2012.10.019

Arah, J., & Smith, K. (1989). Steady-state denitrification in aggregated soils: A mathematical model. *Journal of Soil Science*, *40*(1), 139–149. https://doi.org/10.1111/j.1365-2389.1989.tb01262.x

Augustin, J., Merbach, W., & Rogasik, J. (1998). Factors influencing nitrous oxide and methane emissions from minerotrophic fens in northeast Germany. In *Biology and fertility of soils* (Vol. 28, pp. 1–4).

Azam, F. (1998). Microbial control of oceanic carbon flux: The plot thickens. *Science*, *280*(5364), 694–696. https://doi.org/10.1126/science.280.5364.694

Baldocchi, D. (2014). Measuring fluxes of trace gases and energy between ecosystems and the atmosphere—The state and future of the eddy covariance method. *Global Change Biology*, *20*(12), 3600–3609. https://doi.org/10.1111/gcb.12649

Bardgett, R. D., Freeman, C., & Ostle, N. J. (2008). Microbial contributions to climate change through carbon cycle feedbacks. *The ISME Journal*, *2*(8), 805–814. https://doi.org/10.1038/ismej.2008.58

Borer, B., Tecon, R., & Or, D. (2018). Spatial organization of bacterial populations in response to oxygen and carbon counter-gradients in pore networks. *Nature Communications*, *9*(1), 769. https://doi.org/10.1038/s41467-018-03187-y

Bousquet, P., Ciais, P., Miller, J. B., Dlugokencky, E. J., Hauglustaine, D. A., Prigent, C., et al. (2006). Contribution of anthropogenic and natural sources to atmospheric methane variability. *Nature*, *443*(7110), 439–443. https://doi.org/10.1038/nature05132

Bouwman, A. F. (1998). Environmental science: Nitrogen oxides and tropical agriculture. *Nature*, *392*(6679), 866–867. https://doi.org/10.1038/31809

Bradford, M. A., & Fierer, N. (2012). The biogeography of microbial communities and ecosystem processes: Implications for soil and ecosystem models. In *Soil ecology and ecosystem services*, (pp. 189–200). https://doi.org/10.1093/acprof:oso/9780199575923.003.0017

Briar, S. S., Fonte, S. J., Park, I., Six, J., Scow, K., & Ferris, H. (2011). The distribution of nematodes and soil microbial communities across soil aggregate fractions and farm management systems. *Soil Biology and Biochemistry*, *43*(5), 905–914. https://doi.org/10.1016/j.soilbio.2010.12.017

Butterbach-Bahl, K., Baggs, E. M., Dannenmann, M., Kiese, R., & Zechmeister-Boltenstern, S. (2013). Nitrous oxide emissions from soils: How well do we understand the processes and their controls? *Philosophical Transactions of the Royal Society of London. Series B, Biological Sciences*, *368*(1621), 20130122. https://doi.org/10.1098/rstb.2013.0122

Clark, M. P., Nijssen, B., Lundquist, J. D., Kavetski, D., Rupp, D. E., Woods, R. A., et al. (2015). A unified approach for process-based hydrologic modeling: 1. Modeling concept. *Water Resources Research*, *51*, 2498–2514. https://doi.org/10.1002/2015WR017198

Currie, J. A. (1962). Gaseous diffusion in the aeration of aggregated soil. *Soil Science*, *92*, 40–45.

Cosentino, D., Chenu, C., & Le Bissonnais, Y. (2006). Aggregate stability and microbial community dynamics under drying-wetting cycles in a silt loam soil. *Soil Biology and Biochemistry*, *38*(8), 2053–2062. https://doi.org/10.1016/j.soilbio.2005.12.022

Davidson, E. A. (1991). Fluxes of nitrous oxide and nitric oxide from terrestrial ecosystems. In *Microbial production and consumption of greenhouse gases: Methane, nitrogen oxides, and halomethanes*, (pp. 219–235).

Davidson, E. A., Belk, E., & Boone, R. D. (1998). Soil water content and temperature as independent or confounded factors controlling soil respiration in a temperate mixed hardwood forest. *Global Change Biology*, *4*(2), 217–227. https://doi.org/10.1046/j.1365-2486.1998.00128.x

Davidson, E. A., Janssens, I. A., & Lou, Y. (2006). On the variability of respiration in terrestrial ecosystems: Moving beyond Q_{10}. *Global Change Biology*, *12*(2), 154–164. https://doi.org/10.1111/j.1365-2486.2005.01065.x

Davidson, E. A., Savage, K. E., & Finzi, A. C. (2014). A big-microsite framework for soil carbon modeling. *Global Change Biology*, *20*(12), 3610–3620. https://doi.org/10.1111/gcb.12718

Drake, J. E., Darby, B. A., Giasson, M.-A., Kramer, M. A., Phillips, R. P., & Finzi, A. C. (2013). Stoichiometry constrains microbial response to root exudation—Insights from a model and a field experiment in a temperate forest. *Biogeosciences*, *10*(2), 821–838. https://doi.org/10.5194/bg-10-821-2013

Ebrahimi, A. (2017). *Microbial life in unsaturated soil pore networks—Trophic interactions and dispersal processes*. Switzerland: ETH Zurich.

Ebrahimi, A., & Or, D. (2015). Hydration and diffusion processes shape microbial community organization and function in model soil aggregates. *Water Resources Research*, *51*, 9804–9827. https://doi.org/10.1002/2015WR017565

Ebrahimi, A., & Or, D. (2016). Microbial community dynamics in soil aggregates shape biogeochemical gas fluxes from soil profiles—Upscaling an aggregate biophysical model. *Global Change Biology*, *22*(9), 3141–3156. https://doi.org/10.1111/gcb.13345

Ebrahimi, A., & Or, D. (2017). Mechanistic modeling of microbial interactions at pore to profile scale resolve methane emission dynamics from permafrost soil. *Journal of Geophysical Research: Biogeosciences*, *122*, 1216–1238. https://doi.org/10.1002/2016JG003674

Ebrahimi, A., & Or, D. (2018). Dynamics of soil biogeochemical gas emissions shaped by remolded aggregate sizes and carbon configurations under hydration cycles. *Global Change Biology*, *24*(1), e378–e392. https://doi.org/10.1111/gcb.13938

Ebrahimi, A. N., & Or, D. (2014). Microbial dispersal in unsaturated porous media: Characteristics of motile bacterial cell motions in unsaturated angular pore networks. *Water Resources Research*, *50*, 7406–7429. https://doi.org/10.1002/2014WR015897

Elberling, B., Christiansen, H. H., & Hansen, B. U. (2010). High nitrous oxide production from thawing permafrost. *Nature Geoscience*, *3*(7), 506–506. https://doi.org/10.1038/ngeo893

Elliott, E. T. (1986). Aggregate structure and carbon, nitrogen, and phosphorus in native and cultivated soils. *Soil Science Society of America Journal*, *50*(3), 627–633. https://doi.org/10.2136/sssaj1986.03615995005000030017x

Fierer, N., Schimel, J. P., & Holden, P. A. (2003). Influence of drying–rewetting frequency on soil bacterial community structure. *Microbial Ecology*, *45*(1), 63–71. https://doi.org/10.1007/s00248-002-1007-2

Fierer, N., Strickland, M. S., Liptzin, D., Bradford, M. A., & Cleveland, C. C. (2009). Global patterns in belowground communities. *Ecology Letters*, *12*(11), 1238–1249. https://doi.org/10.1111/j.1461-0248.2009.01360.x

Foley, J. A., Prentice, I. C., Ramankutty, N., Levis, S., Pollard, D., Sitch, S., & Haxeltine, A. (1996). An integrated biosphere model of land surface processes, terrestrial carbon balance, and vegetation dynamics. *Global Biogeochemical Cycles*, *10*(4), 603–628. https://doi.org/10.1029/96GB02692

Gardner, W. R. (1956). Representation of soil aggregate-size distribution by a logarithmic-normal distribution. *Soil Science Society of America Journal*, *20*(2), 151. https://doi.org/10.2136/sssaj1956.03615995002000020003x

Gil, J., Pérez, T., Boering, K., Martikainen, P. J., & Biasi, C. (2017). Mechanisms responsible for high N_2O emissions from subarctic permafrost peatlands studied via stable isotope techniques. *Global Biogeochemical Cycles*, *31*, 172–189. https://doi.org/10.1002/2015GB005370

Goldberg, S. D., Knorr, K. H., Blodau, C., Lischeid, G., & Gebauer, G. (2010). Impact of altering the water table height of an acidic fen on N_2O and NO fluxes and soil concentrations. *Global Change Biology*, *16*(1), 220–233. https://doi.org/10.1111/j.1365-2486.2009.02015.x

Gorham, E. (1991). Northern peatlands: Role in the carbon cycle and probable responses to climatic warming. *Ecological Applications*, *1*(2), 182–195. https://doi.org/10.2307/1941811

Graham, D. E., Wallenstein, M. D., Vishnivetskaya, T. A., Waldrop, M. P., Phelps, T. J., Pfiffner, S. M., et al. (2012). Microbes in thawing permafrost: The unknown variable in the climate change equation. *The ISME Journal*, *6*(4), 709–712. https://doi.org/10.1038/ismej.2011.163

Griffis, T. J., Chen, Z., Baker, J. M., Wood, J. D., Millet, D. B., Lee, X., et al. (2017). Nitrous oxide emissions are enhanced in a warmer and wetter world. *Proceedings of the National Academy of Sciences of the United States of America*, *114*(45), 12,081–12,085.

Groffman, P., Butterbach-Bahl, K., Fulweiler, R., Gold, A., Morse, J., Stander, E., et al. (2009). Challenges to incorporating spatially and temporally explicit phenomena (hotspots and hot moments) in denitrification models. *Biogeochemistry*, *93*(1–2), 49–77. https://doi.org/10.1007/s10533-008-9277-5

Gupta, V. V. S. R., & Germida, J. J. (2015). Soil aggregation: Influence on microbial biomass and implications for biological processes. *Soil Biology and Biochemistry*, *80*, A3–A9. https://doi.org/10.1016/j.soilbio.2014.09.002

Haghighi, E., Shahraeeni, E., Lehmann, P., & Or, D. (2013). Evaporation rates across a convective air boundary layer are dominated by diffusion. *Water Resources Research*, *49*, 1602–1610. https://doi.org/10.1002/wrcr.20166

Hansen, J., Sato, M., Ruedy, R., Lacis, A., & Oinas, V. (2000). Global warming in the twenty-first century: An alternative scenario. *Proceedings of the National Academy of Sciences*, *97*(18), 9875–9880. https://doi.org/10.1073/pnas.170278997

Hawkes, C. V., & Keitt, T. H. (2015). Resilience vs. historical contingency in microbial responses to environmental change. *Ecology Letters*, *18*(7), 612–625. https://doi.org/10.1111/ele.12451

He, Y., Zhuang, Q., Harden, J. W., McGuire, A. D., Fan, Z., Liu, Y., & Wickland, K. P. (2014). The implications of microbial and substrate limitation for the fates of carbon in different organic soil horizon types of boreal forest ecosystems: A mechanistically based model analysis. *Biogeosciences*, *11*(16), 4477–4491. https://doi.org/10.5194/bg-11-4477-2014

Hengl, T., Mendes de Jesus, J., Heuvelink, G. B. M., Ruiperez Gonzalez, M., Kilibarda, M., Blagotić, A., et al. (2017). SoilGrids250m: Global gridded soil information based on machine learning. *PLoS One*, *12*(2), e0169748. https://doi.org/10.1371/journal.pone.0169748

Horn, R., Stepniewski, W., Wlodarczyk, T., Walenzik, G., & Eckhardt, F. E. W. (1994). Denitrification rate and microbial distribution within homogeneous model soil aggregates. *International Agrophysics*, *8*(1), 65–74.

House, A. R., Thompson, J. R., & Acreman, M. C. (2016). Projecting impacts of climate change on hydrological conditions and biotic responses in a chalk valley riparian wetland. *Journal of Hydrology*, *534*, 178–192. https://doi.org/10.1016/j.jhydrol.2016.01.004

Huffman, G. J., Bolvin, D. T., & Adler, R. F. (2016). GPCP Version 1.2 One-Degree Daily Precipitation Data Set, https://doi.org/10.5065/D6D50K46, Research Data Archive at the National Center for Atmospheric Research, Computational and Information Systems Laboratory, Boulder, CO. (Updated irregularly.)

Hugelius, G., Virtanen, T., Kaverin, D., Pastukhov, A., Rivkin, F., Marchenko, S., et al. (2011a). High-resolution mapping of ecosystem carbon storage and potential effects of permafrost thaw in periglacial terrain, European Russian Arctic. *Journal of Geophysical Research*, *116*, G03024. https://doi.org/10.1029/2010JG001606

Hugelius, G., Virtanen, T., Kaverin, D., Pastukhov, A., Rivkin, F., Marchenko, S., et al. (2011b). High-resolution mapping of ecosystem carbon storage and potential effects of permafrost thaw in periglacial terrain, European Russian Arctic. *Journal of Geophysical Research*, *116*, G03024. https://doi.org/10.1029/2010JG001606

IPCC (2014). Climate change 2014 synthesis report, Contrib. Work. Groups I, II III to fifth assess. Rep. Intergov. Panel. *Climatic Change*, 1–151. https://doi.org/10.1017/CBO9781107415324

Jansson, J. K., & Taş, N. (2014). The microbial ecology of permafrost. *Nature Reviews Microbiology*, *12*(6), 414–425. https://doi.org/10.1038/nrmicro3262

Kim, M., & Or, D. (2016). Individual-based model of microbial life on hydrated rough soil surfaces. *PLoS One*, *11*(1), e0147394. https://doi.org/10.1371/journal.pone.0147394

Kim, M., & Or, D. (2017). Hydration status and diurnal trophic interactions shape microbial community function in desert biocrusts. *Biogeosciences*, *14*(23), 5403–5424. https://doi.org/10.5194/bg-14-5403-2017

Kunkel, K. E., Karl, T. R., Easterling, D. R., Redmond, K., Young, J., Yin, X., & Hennon, P. (2013). Probable maximum precipitation and climate change. *Geophysical Research Letters*, *40*, 1402–1408. https://doi.org/10.1002/grl.50334

Kuzyakov, Y., & Blagodatskaya, E. (2015). Microbial hotspots and hot moments in soil: Concept & review. *Soil Biology and Biochemistry*, *83*, 184–199. https://doi.org/10.1016/j.soilbio.2015.01.025

Liengaard, L., Nielsen, L. P., Revsbech, N. P., Priemé, A., Elberling, B., Enrich-Prast, A., & Kühl, M. (2012). Extreme emission of N_2O from tropical wetland soil (Pantanal, South America). *Frontiers in Microbiology*, *3*(JAN). https://doi.org/10.3389/fmicb.2012.00433

Liljedahl, A. K., Boike, J., Daanen, R. P., Fedorov, A. N., Frost, G. V., Grosse, G., et al. (2016). Pan-Arctic ice-wedge degradation in warming permafrost and its influence on tundra hydrology. *Nature Geoscience*, *9*(4), 312–318.

Manzoni, S., Moyano, F., Kätterer, T., & Schimel, J. (2016). Modeling coupled enzymatic and solute transport controls on decomposition in drying soils. *Soil Biology and Biochemistry*, *95*, 275–287. https://doi.org/10.1016/j.soilbio.2016.01.006

Manzoni, S., & Porporato, A. (2009). Soil carbon and nitrogen mineralization: Theory and models across scales. *Soil Biology and Biochemistry*, *41*(7), 1355–1379. https://doi.org/10.1016/j.soilbio.2009.02.031

Manzoni, S., Schaeffer, S. M., Katul, G., Porporato, A., & Schimel, J. P. (2014). A theoretical analysis of microbial eco-physiological and diffusion limitations to carbon cycling in drying soils. *Soil Biology and Biochemistry*, *73*, 69–83. https://doi.org/10.1016/j.soilbio.2014.02.008

Manzoni, S., Taylor, P., Richter, A., Porporato, A., & Ågren, G. I. (2012). Environmental and stoichiometric controls on microbial carbon-use efficiency in soils. *The New Phytologist*, *196*(1), 79–91. https://doi.org/10.1111/j.1469-8137.2012.04225.x

Markfoged, R., Nielsen, L. P., Nyord, T., Ottosen, L. D. M., & Revsbech, N. P. (2011). Transient N_2O accumulation and emission caused by O_2 depletion in soil after liquid manure injection. *European Journal of Soil Science*, *62*(4), 541–550. https://doi.org/10.1111/j.1365-2389.2010.01345.x

Martikainen, P. J., Nykanen, H., Crill, P., & Silvola, J. (1993). Effect of a lowered water table on nitrous oxide fluxes from northern peatlands. *Nature*, *366*(6450), 51–53. https://doi.org/10.1038/366051a0

Marushchak, M. E., Pitkämäki, A., Koponen, H., Biasi, C., Seppälä, M., & Martikainen, P. J. (2011). Hot spots for nitrous oxide emissions found in different types of permafrost peatlands. *Global Change Biology*, *17*(8), 2601–2614. https://doi.org/10.1111/j.1365-2486.2011.02442.x

McClain, M. E., Boyer, E. W., Dent, C. L., Gergel, S. E., Grimm, N. B., Groffman, P. M., et al. (2003). Biogeochemical hot spots and hot moments at the interface of terrestrial and aquatic ecosystems. *Ecosystems*, *6*(4), 301–312. https://doi.org/10.1007/s10021-003-0161-9

McGuire, A. D., Sitch, S., Clein, J. S., Dargaville, R., Esser, G., Foley, J., et al. (2001). Carbon balance of the terrestrial biosphere in the twentieth century: Analyses of CO_2, climate and land use effects with four process-based ecosystem models. *Global Biogeochemical Cycles*, *15*(1), 183–206. https://doi.org/10.1029/2000GB001298

Meinshausen, M., Meinshausen, N., Hare, W., Raper, S. C. B., Frieler, K., Knutti, R., et al. (2009). Greenhouse-gas emission targets for limiting global warming to 2 °C. *Nature*, *458*(7242), 1158–1162. https://doi.org/10.1038/nature08017

Molina-Herrera, S., Haas, E., Klatt, S., Kraus, D., Augustin, J., Magliulo, V., et al. (2016). A modeling study on mitigation of N_2O emissions and NO_3 leaching at different agricultural sites across Europe using LandscapeDNDC. *Science of The Total Environment*, *553*(3), 128–140. https://doi.org/10.1016/j.scitotenv.2015.12.099

Morales, S. E., Cosart, T., & Holben, W. E. (2010). Bacterial gene abundances as indicators of greenhouse gas emission in soils. *The ISME Journal*, *4*(6), 799–808. https://doi.org/10.1038/ismej.2010.8

Morley, N., & Baggs, E. M. (2010). Carbon and oxygen controls on N_2O and N_2 production during nitrate reduction. *Soil Biology and Biochemistry*, *42*(10), 1864–1871. https://doi.org/10.1016/j.soilbio.2010.07.008

Morley, N., Baggs, E. M., Dörsch, P., & Bakken, L. (2008). Production of NO, N_2O and N_2 by extracted soil bacteria, regulation by NO_2^- and O_2 concentrations. *FEMS Microbiology Ecology*, *65*(1), 102–112. https://doi.org/10.1111/j.1574-6941.2008.00495.x

Murguia-Flores, F., Arndt, S., Ganesan, A. L., Murray-Tortarolo, G. N., & Hornibrook, E. R. C. (2017). Soil methanotrophy model (MeMo v1.0): A process-based model to quantify global uptake of atmospheric methane by soil. *Geoscientific Model Development Discussion*, 1–38. https://doi.org/10.5194/gmd-2017-124

Natali, S. M., Schuur, E. A. G., Trucco, C., Hicks Pries, C. E., Crummer, K. G., & Baron Lopez, A. F. (2011). Effects of experimental warming of air, soil and permafrost on carbon balance in Alaskan tundra. *Global Change Biology*, *17*(3), 1394–1407. https://doi.org/10.1111/j.1365-2486.2010.02303.x

Nie, M., Pendall, E., Bell, C., & Wallenstein, M. D. (2014). Soil aggregate size distribution mediates microbial climate change feedbacks. *Soil Biology and Biochemistry*, *68*, 357–365. https://doi.org/10.1016/j.soilbio.2013.10.012

Nishimura, S., Yonemura, S., Minamikawa, K., & Yagi, K. (2015). Seasonal and diurnal variations in net carbon dioxide flux throughout the year from soil in paddy field. *Journal of Geophysical Research: Biogeosciences*, *120*, 63–76. https://doi.org/10.1002/2014JG002746

Nunan, N., Wu, K., Young, I. M., Crawford, J. W., & Ritz, K. (2003). Spatial distribution of bacterial communities and their relationships with the micro-architecture of soil. *FEMS Microbiology Ecology*, *44*(2), 203–215. https://doi.org/10.1016/S0168-6496(03)00027-8

Nunan, N., Young, I., Crawford, J., & Ritz, K. (2007). Bacterial interactions at the microscale—Linking habitat to function in soil. In R. Franklin, & A. Mills (Eds.), *The spatial distribution of microbes in the environment SE - 3* (pp. 61–85). Berlin: Springer.

Oberman, N., & Mazhitova, G. (2001). Permafrost dynamics in the north-east of European Russia at the end of the 20th century. *Norwegian Journal of Geography*, *55*(4), 241–244. https://doi.org/10.1080/00291950152746595

Or, D., Smets, B. F., Wraith, J. M., Dechesne, A., & Friedman, S. P. (2007). Physical constraints affecting bacterial habitats and activity in unsaturated porous media—A review. *Advances in Water Resources*, *30*(6–7), 1505–1527. https://doi.org/10.1016/j.advwatres.2006.05.025

Philippot, L. (1996). Dissimilatory nitrite-reductase provides a competitive advantage to *Pseudomonas* sp. RTC01 to colonise the centre of soil aggregates. *FEMS Microbiology Ecology*, *21*(3), 175–185. https://doi.org/10.1016/S0168-6496(96)00054-2

Pinheiro, E. F. M., Pereira, M. G., & Anjos, L. H. C. (2004). Aggregate distribution and soil organic matter under different tillage systems for vegetable crops in a red latosol from Brazil. *Soil and Tillage Research*, *77*(1), 79–84. https://doi.org/10.1016/j.still.2003.11.005

Pomeroy, J. W., Gray, D. M., Brown, T., Hedstrom, N. R., Quinton, W. L., Granger, R. J., & Carey, S. K. (2007). The cold regions hydrological model: A platform for basing process representation and model structure on physical evidence. *Hydrological Processes*, *21*, 2650–2667.

Pumpanen, J., Ilvesniemi, H., & Hari, P. (2003). A process-based model for predicting soil carbon dioxide efflux and concentration. *Soil Science Society of America Journal*, *67*(2), 402–413. https://doi.org/10.2136/sssaj2003.4020

Rabot, E., Lacoste, M., Hénault, C., & Cousin, I. (2015). Using X-ray computed tomography to describe the dynamics of nitrous oxide emissions during soil drying. *Vadose Zone Journal*, *14*(8). https://doi.org/10.2136/vzj2014.12.0177

Regina, K., Nykänen, H., Silvola, J., & Martikainen, P. J. (1996). Fluxes of nitrous oxide from boreal peatlands as affected by peatland type, water table level and nitrification capacity. *Biogeochemistry*, *35*(3), 401–418. https://doi.org/10.1007/BF02183033

Repo, M. E., Susiluoto, S., Lind, S. E., Jokinen, S., Elsakov, V., Biasi, C., et al. (2009). Large N_2O emissions from cryoturbated peat soil in tundra. *Nature Geoscience*, *2*(3), 189–192. https://doi.org/10.1038/NGEO434

Robertson, G. P., & tiedje, J. M. (1987). Nitrous oxide sources in aerobic soils: Nitrification, denitrification and other biological processes. *Soil Biology and Biochemistry*, *19*(2), 187–193. https://doi.org/10.1016/0038-0717(87)90080-0

Romanovsky, V. E., Drozdov, D. S., Oberman, N. G., Malkova, G. V., Kholodov, A. L., Marchenko, S. S., et al. (2010). Thermal state of permafrost in Russia. *Permafrost and Periglacial Processes*, *21*(2), 136–155. https://doi.org/10.1002/ppp.683

Schimel, J. (2001). 1.13 - *Biogeochemical models: Implicit versus explicit microbiology BT—Global biogeochemical cycles in the climate system* (pp. 177–183). San Diego, CA: Academic Press.

Schimel, J. P., & Schaeffer, S. M. (2012). Microbial control over carbon cycling in soil. *Frontiers in Microbiology*, *3*. https://doi.org/10.3389/fmicb.2012.00348

Schipper, L. A., Hobbs, J. K., Rutledge, S., & Arcus, V. L. (2014). Thermodynamic theory explains the temperature optima of soil microbial processes and high Q_{10} values at low temperatures. *Global Change Biology*, *20*(11), 3578–3586. https://doi.org/10.1111/gcb.12596

Schrenk, K. J., Araújo, N. A. M., Andrade, J. S., & Herrmann, H. J. (2012). Fracturing ranked surfaces. *Scientific Reports*, *2*(1), 348. https://doi.org/10.1038/srep00348

Schweizer, S. A., Hoeschen, C., Schlüter, S., Kögel-Knabner, I., & Mueller, C. W. (2018). Rapid soil formation after glacial retreat shaped by spatial patterns of organic matter accrual in microaggregates. *Global Change Biology*, *24*(4), 1637–1650. https://doi.org/10.1111/gcb.14014

Scott-Denton, L. E., Sparks, K. L., & Monson, R. K. (2003). Spatial and temporal controls of soil respiration rate in a high-elevation, subalpine forest. *Soil Biology and Biochemistry*, *35*(4), 525–534. https://doi.org/10.1016/S0038-0717(03)00007-5

Sexstone, A. J., Revsbech, N. P., Parkin, T. B., & Tiedje, J. M. (1985). Direct measurement of oxygen profiles and denitrification rates in soil aggregates. *Soil Science Society of America Journal*, *49*(3), 645. https://doi.org/10.2136/sssaj1985.03615995004900030024x

Shahraeeni, E., & Or, D. (2012). Pore scale mechanisms for enhanced vapor transport through partially saturated porous media. *Water Resources Research*, *48*, W05511. n/a-n/a, https://doi.org/10.1029/2011WR011036

Shurpali, N. J., Rannik, Ü., Jokinen, S., Lind, S., Biasi, C., Mammarella, I., et al. (2016). Neglecting diurnal variations leads to uncertainties in terrestrial nitrous oxide emissions. *Scientific Reports*, *6*(1), 25739. https://doi.org/10.1038/srep25739

Sierra, C. A., Harmon, M. E., & Perakis, S. S. (2011). Decomposition of heterogeneous organic matter and its long-term stabilization in soils. *Ecological Monographs*, *81*(4), 619–634. https://doi.org/10.1890/11-0811.1

Sierra, C. A., Müller, M., & Trumbore, S. E. (2012). Models of soil organic matter decomposition: The SoilR package, version 1.0. *Geoscientific Model Development*, *5*(4), 1045–1060. https://doi.org/10.5194/gmd-5-1045-2012

Simunek, J., Van Genuchten, M., & Sejna, M. (2012). HYDRUS: Model use, calibration, and validation. *Transactions of the ASABE*, *55*(1987), 1261–1274. https://doi.org/10.1029/2002WR001340

Sitch, S., Huntingford, C., Gedney, N., Levy, P. E., Lomas, M., Piao, S. L., et al. (2008). Evaluation of the terrestrial carbon cycle, future plant geography and climate-carbon cycle feedbacks using five dynamic global vegetation models (DGVMs). *Global Change Biology*, *14*, 2015–2039. https://doi.org/10.1111/j.1365-2486.2008.01626.x

Six, J., Elliott, E. T., Paustian, K., & Doran, J. W. (1998). Aggregation and soil organic matter accumulation in cultivated and native grassland soils. *Soil Science Society of America Journal*, *62*(5), 1367. https://doi.org/10.2136/sssaj1998.03615995006200050032x

Smith, J. U., Smith, P., Monaghan, R., & MacDonald, A. J. (2002). When is a measured soil organic matter fraction equivalent to a model pool? *European Journal of Soil Science*, *53*(3), 405–416. https://doi.org/10.1046/j.1365-2389.2002.00458.x

Smith, K. A. (1980). A model of the extent of anaerobic zones in aggregated soils, and its potential application to estimates of denitrification. *Journal of Soil Science*, *31*(2), 263–277. https://doi.org/10.1111/j.1365-2389.1980.tb02080.x

Tang, J., & Baldocchi, D. D. (2005). Spatial–temporal variation in soil respiration in an oak–grass savanna ecosystem in California and its partitioning into autotrophic and heterotrophic components. *Biogeochemistry*, *73*(1), 183–207. https://doi.org/10.1007/s10533-004-5889-6

Taylor, R. G., Scanlon, B., Döll, P., Rodell, M., van Beek, R., Wada, Y., et al. (2013). Ground water and climate change. *Nature Climate Change*, *3*(4), 322–329. https://doi.org/10.1038/nclimate1744

Tecon, R., & Or, D. (2017). Cooperation in carbon source degradation shapes spatial self-organization of microbial consortia on hydrated surfaces. *Scientific Reports*, *7*, 43726. https://doi.org/10.1038/srep43726

Tiedje, J. M., Sexstone, A. J., Myrold, D. D., & Robinson, J. A. (1983). Denitrification: Ecological niches, competition and survival. *Antonie Van Leeuwenhoek*, *48*(6), 569–583. https://doi.org/10.1007/BF00399542

Tiedje, J. M., Sexstone, A. J., Parkin, T. B., & Revsbech, N. P. (1984). Anaerobic processes in soil. *Plant and Soil*, *76*(1–3), 197–212. https://doi.org/10.1007/BF02205580

Tóth, B., Weynants, M., Nemes, A., Makó, A., Bilas, G., & Tóth, G. (2015). New generation of hydraulic pedotransfer functions for Europe. *European Journal of Soil Science*, *66*(1), 226–238. https://doi.org/10.1111/ejss.12192

Totsche, K. U., Amelung, W., Gerzabek, M. H., Guggenberger, G., Klumpp, E., Knief, C., et al. (2018). Microaggregates in soils. *Journal of Plant Nutrition and Soil Science*, *181*(1), 104–136. https://doi.org/10.1002/jpln.201600451

Townsend, A. R., Asner, G. P., & Cleveland, C. C. (2008). The biogeochemical heterogeneity of tropical forests. *Trends in Ecology & Evolution*, *23*(8), 424–431. https://doi.org/10.1016/j.tree.2008.04.009

Trenberth, K. E. (2011). Changes in precipitation with climate change. *Climate Research*, *47*(1), 123–138. https://doi.org/10.3354/cr00953

Vogel, L. E., Makowski, D., Garnier, P., Vieublé-Gonod, L., Coquet, Y., Raynaud, X., et al. (2015). Modeling the effect of soil meso- and macropores topology on the biodegradation of a soluble carbon substrate. *Advances in Water Resources*, *83*, 123–136. https://doi.org/10.1016/j.advwatres.2015.05.020

Voigt, C., Lamprecht, R. E., Marushchak, M. E., Lind, S. E., Novakovskiy, A., Aurela, M., et al. (2016). Warming of subarctic tundra increases emissions of all three important greenhouse gases—Carbon dioxide, methane, and nitrous oxide. *Global Change Biology*, *23*, 3121–3138. https://doi.org/10.1111/gcb.13563

Wang, G., & Or, D. (2014). Trophic interactions induce spatial self-organization of microbial consortia on rough surfaces. *Scientific Reports*, *4*(1), 6757. https://doi.org/10.1038/srep06757

Wang, J., Song, C., Zhang, J., Wang, L., Zhu, X., & Shi, F. (2014). Temperature sensitivity of soil carbon mineralization and nitrous oxide emission in different ecosystems along a mountain wetland-forest ecotone in the continuous permafrost of Northeast China. *Catena*, *121*, 110–118. https://doi.org/10.1016/j.catena.2014.05.007

Wieder, W. R., Allison, S. D., Davidson, E. A., Georgiou, K., Hararuk, O., He, Y., et al. (2015). Explicitly representing soil microbial processes in Earth system models. *Global Biogeochemical Cycles*, *29*, 1782–1800. https://doi.org/10.1002/2015GB005188

Wieder, W. R., Grandy, A. S., Kallenbach, C. M., & Bonan, G. B. (2014). Integrating microbial physiology and physio-chemical principles in soils with the MIcrobial-MIneral Carbon Stabilization (MIMICS) model. *Biogeosciences*, *11*(14), 3899–3917. https://doi.org/10.5194/bg-11-3899-2014

Wu, L., Rees, R. M., Tarsitano, D., Zhang, X., Jones, S. K., & Whitmore, A. P. (2015). Simulation of nitrous oxide emissions at field scale using the SPACSYS model. *Science of the Total Environment*, *530-531*, 76–86. https://doi.org/10.1016/j.scitotenv.2015.05.064

Young, I. M., & Crawford, J. W. (2004). Interactions and self-organization in the soil-microbe complex. *Science*, *304*(5677), 1634–1637. https://doi.org/10.1126/science.1097394

Zona, D., Gioli, B., Commane, R., Lindaas, J., Wofsy, S. C., Miller, C. E., et al. (2016). Cold season emissions dominate the Arctic tundra methane budget. *Proceedings of the National Academy of Sciences*, *113*(1), 40–45. https://doi.org/10.1073/pnas.1516017113